Part IV

Large network, less details

ODE modeling of evidence-based extrinsic apoptosis network

Week 9

The extensive studies of an extrinsic apoptotic reaction model

OPEN ACCESS Freely available online

PLoS BIOLOGY

Modeling a Snap-Action, Variable-Delay Switch Controlling Extrinsic Cell Death

John G. Albeck[1], John M. Burke[1,2], Sabrina L. Spencer[1,3], Douglas A. Lauffenburger[2,3], Peter K. Sorger[1,2*]

1 Department of Systems Biology, Harvard Medical School, Boston, Massachusetts, United States of America, 2 Biological Engineering Department, Massachusetts Institute of Technology, Cambridge, Massachusetts, United States of America, 3 Computational and Systems Biology Initiative, Massachusetts Institute of Technology, Cambridge, Massachusetts, United States of America

When exposed to tumor necrosis factor (TNF) or TNF-related apoptosis-inducing ligand (TRAIL), a closely related death ligand and investigational therapeutic, cells enter a protracted period of variable duration in which only upstream initiator caspases are active. A subsequent and sudden transition marks activation of the downstream effector caspases that rapidly dismantle the cell. Thus, extrinsic apoptosis is controlled by an unusual variable-delay, snap-action switch that enforces an unambiguous choice between life and death. To understand how the extrinsic apoptosis switch functions in quantitative terms, we constructed a mathematical model based on a mass-action representation of known reaction pathways. The model was trained against experimental data obtained by live-cell imaging, flow cytometry, and immunoblotting of cells perturbed by protein depletion and overexpression. The trained model accurately reproduces the behavior of normal and perturbed cells exposed to TRAIL, making it possible to study switching mechanisms in detail. Model analysis shows, and experiments confirm, that the duration of the delay prior to effector caspase activation is determined by initiator caspase-8 activity and the rates of other reactions lying immediately downstream of the TRAIL receptor. Sudden activation of effector caspases is achieved downstream by reactions involved in permeabilization of the mitochondrial membrane and relocalization of proteins such as Smac. We find that the pattern of interactions among Bcl-2 family members, the partitioning of Smac from its binding partner XIAP, and the mechanics of pore assembly are all critical for snap-action control.

Citation: Albeck JG, Burke JM, Spencer SL, Lauffenburger DA, Sorger PK (2008) Modeling a snap-action, variable-delay switch controlling extrinsic cell death. PLoS Biol 6(12): e299. doi:10.1371/journal.pbio.0060299

Key events in apoptosis cascade

- Essential for the development but is misregulated in diseases as diverse as cancer and autoimmunity
- Activation of the potent effector caspases (caspases-3 and -7), (*C3 and C7)* triggered by:
  - **intrinsic** cell death pathway by intracellular events such as **DNA damage** and **oxidative stress**
  - **extrinsic** cell death pathway by extracellular stimuli such as **TNF** and **TRAIL**
- C3 and C7 directly **degrade the proteome** and, by activating DNAses, also **dismantle the chromosomes** of cells committed to die
- represents an irreversible change in cell fate and is consequently regulated at multiple levels

Previous observations

- Studies of extrinsic apoptosis at the **single-cell** level reveal:
  - **a long and variable delay** prior to effector caspase activation
  - **rapid and sudden progression** to substrate cleavage once activation has begun,
  - a behavior termed "**variable-delay, snap-action**" switching.
  - **failure** in snap-action switching generates an **indeterminate physiological state and sublethal cellular damage** that may predispose cells to **genomic instability**

The quantitative essence of this work

- Theory: constructed a mathematical model based on **a mass-action representation of known reaction pathways**
- Model was trained against **experimental data** perturbed by **protein depletion and overexpression**
- Model **accurately reproduces** the behavior of normal and perturbed cells exposed to TRAIL
- **Model analysis predicts, and experiments confirm:**
  - **duration of the delay prior** to effector caspase activation is determined by initiator caspase-8 activity and other reactions lying immediately downstream of the TRAIL receptor.
  - **sudden activation** of effector caspases is achieved downstream by reactions involved in **permeabilization of the mitochondrial membrane** and relocalization of proteins such as Smac.
- Pattern of interactions among Bcl-2 family members, the partitioning of Smac from its binding partner XIAP, and the mechanics of pore assembly are all critical for snap-action control.

1. Modeling Extrinsic Cell Death Pathways

The network

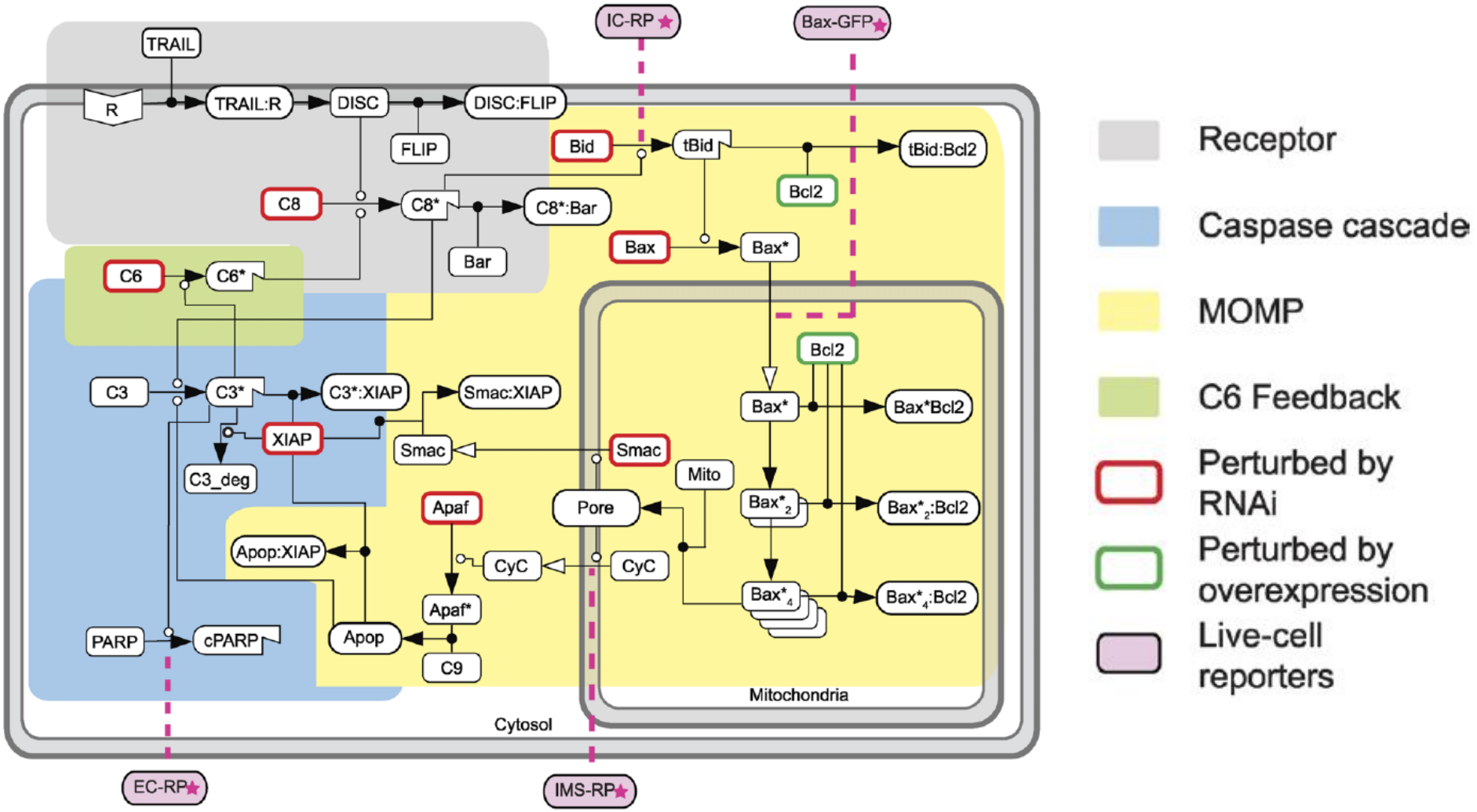

Simplifying: **C8**: C8 and C10; **C3**: C3 and C7;

Bcl-2 family: **Bid**: apoptotic ‘activator’; **Bcl-2**; apoptotic inhibitor

Bax: pore-forming protein

Apoptosis reporters

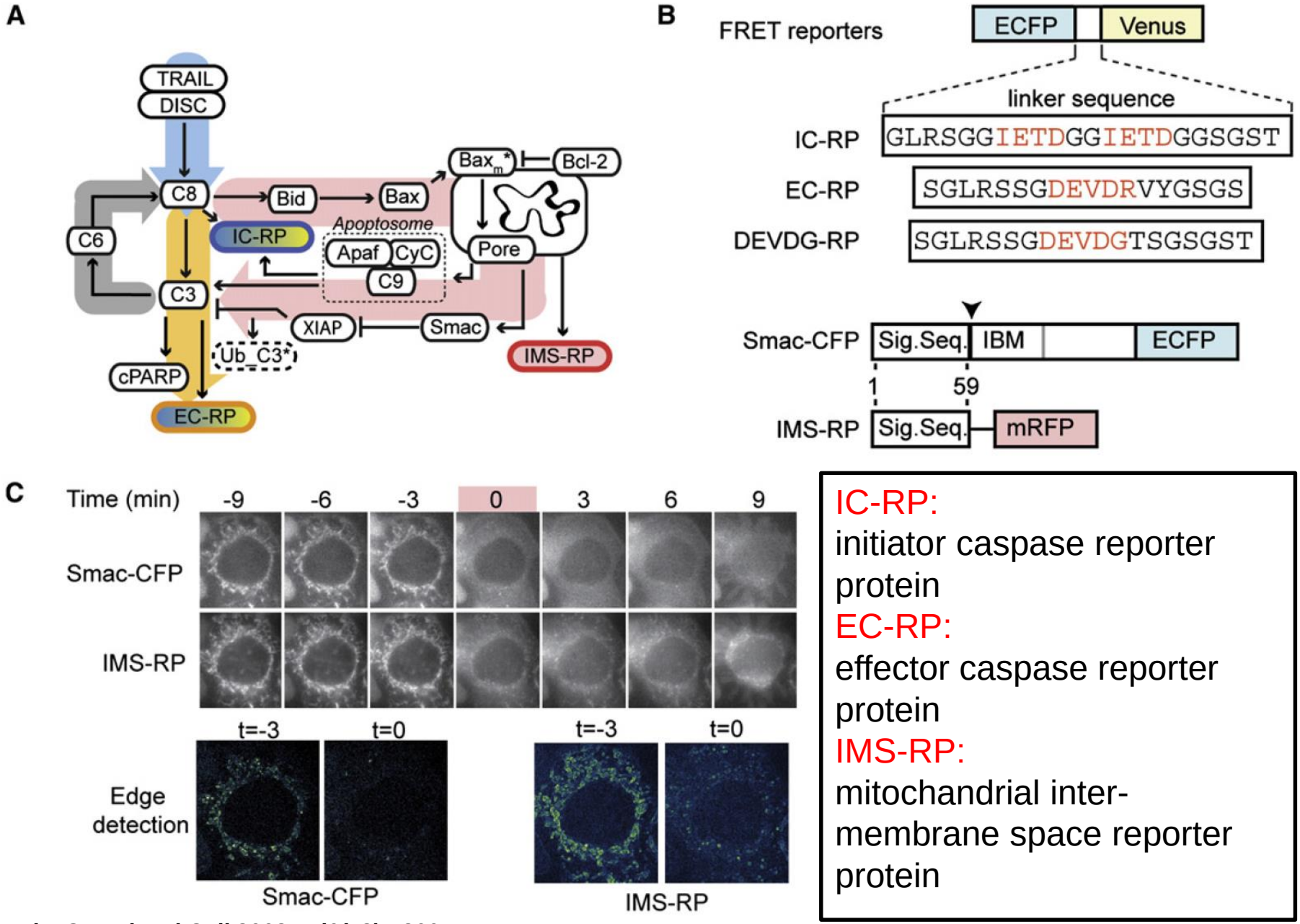

IC-RP:
initiator caspase reporter protein

EC-RP:
effector caspase reporter protein

IMS-RP:
mitochandrial inter-membrane space reporter protein

Albeck JG et al Mol Cell 2008 vol6(12)-e299

Condensed representation

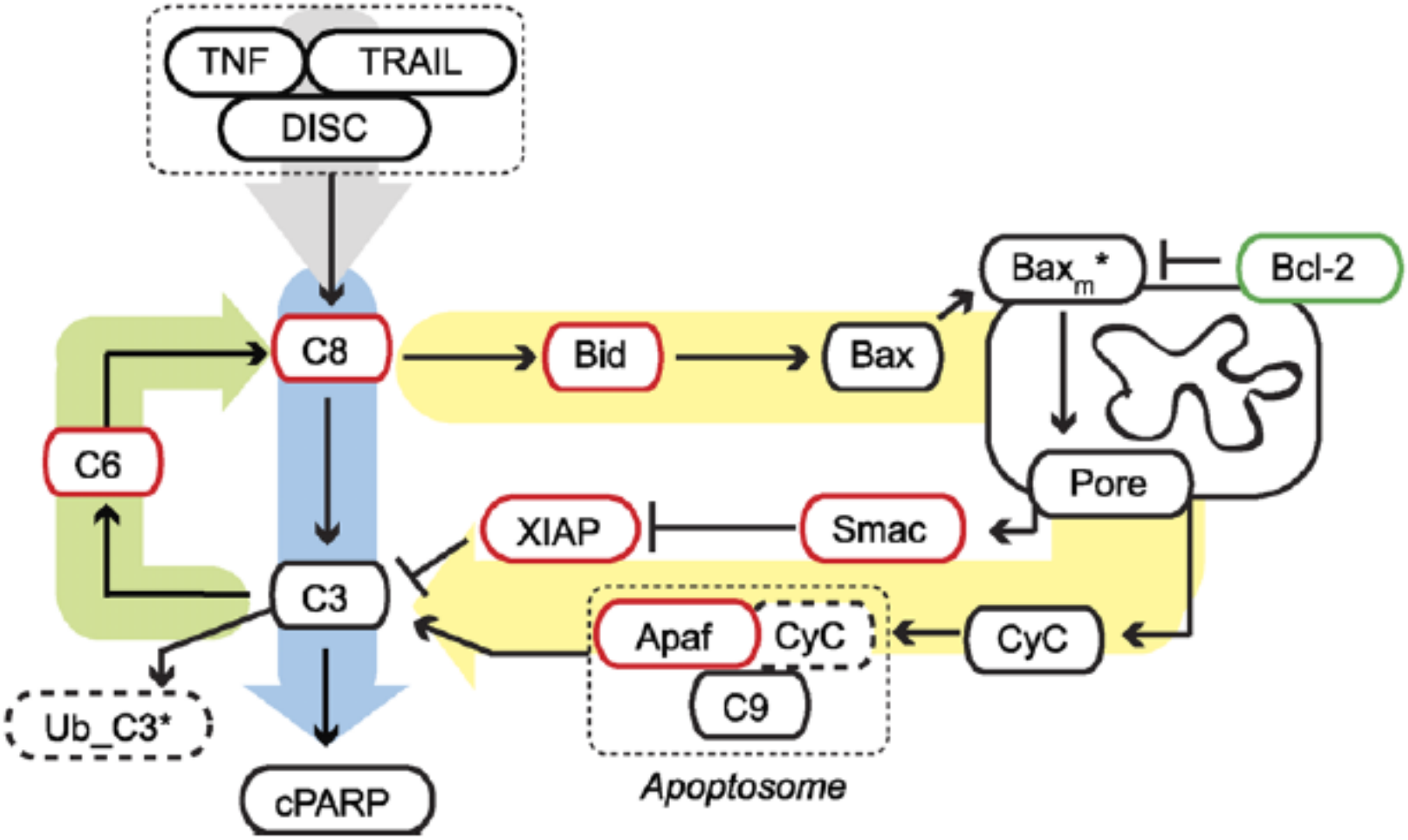

Relevant abbreviations:

C3, caspase-3; **C6**, caspase-6; **C8**, caspase-8; **C9**, caspase-9;
CyC, cytochrome c;
DISC, death-inducing signaling complex;
EARM, extrinsic apoptosis reaction model;
EC-RP, effector caspase reporter protein;
IAP, inhibitor of apoptosis protein;
IC-RP, initiator caspase reporter protein;
IMS-RP, mitochondrial intermembrane space reporter protein;
MOMP, mitochondrial outer membrane permeabilization;
TNF, tumor necrosis factor;
TRAIL, TNF-related apoptosis-inducing ligand

- constructed on the basis of **mass-action kinetics**
- elementary reactions represented as **ODEs**
- all biochemical reaction: **unimolecular or bimolecular reactions**
- Transport : unimolecular reaction
- the assembly of multiprotein complexes as a series of bimolecular reactions
- **ultrasensitivity** and other **nonlinear** behaviors arise from interactions among **simple elementary reactions** (no Hill functions etc)
- Where possible, estimates for **model parameters** (rates and initial protein concentrations) were **obtained from the literature**
- In the absence of such information, parameters were **set to intermediate** values within a physically plausible range and then **fitted** so as to optimize model performance

Table S1. List of Species in EARM v1.0

Species	Description (all species are located in cellular compartment (CC) unless otherwise stated.)
L	death ligand, such as TRAIL and TNF
R	inactive receptor complex
R^*	active receptor complex
$flip$	binds to active receptor acting as an inhibitor
$X:Y = Y:X$	complex formed by species X and Y, for example, $L:R$ is the ligand-receptor complex
$C8$	procaspase-8 and procaspase-10, inactive form of caspase-8 and caspase-10
$C8^*$	cleaved caspase-8 and caspase-10, active form of caspase-8 and caspase-10
Bar	binds to $C8^*$ and acts as an inhibitor
$C3$	procaspase-3 and procaspase-7, inactive form of caspase-3 and caspase-7
$C3^*$	cleaved caspase-3 and caspase-7, active form of caspase-3 and caspase-7
$C6$	procaspase-6, inactive form of caspase-6
$C6^*$	cleaved caspase-6, active form of caspase-6
$XIAP$	X-linked Inhibitor of Apoptosis (XIAP) in the cell
$PARP$	DNA damage repair enzyme, here represents all substrates of $C3^*$
$cPARP$	cleaved $PARP$, measure of single cell death
Bid	substrate of cleaved caspase-8, inactive form
$tBid$	cleaved Bid, active form of Bid
$Bcl2_c$	represents the family of antiapoptotic Bcl-2 proteins in the cellular compartment (CC), it binds to $tBid$ and acts as in inhibitor
Bax	substrate of $tBid$, inactive form
Bax^*	active form of Bax
Bax^*_m	Bax^* in the mitochondrial compartment (MC)
Bax_2	represents $Bax^*_m : Bax^*_m$ in the MC
Bax_4	represents $Bax_2 : Bax_2$ in the MC
$Bcl2$	represents all antiapoptotic Bcl-2 proteins in the MC
M	the number of unoccupied Bax_4 binding sites on outer membrane of the mitochondria, in MC
M^*	the number of pores Bax_4 created on the outer membrane of the mitochondria, in MC
CyC_m	cyotochrome c inside the mitochondria, in MC
CyC_r	cytochrome c released from the mitochondria, but remaining in the MC
CyC	cytochrome c in the CC
$Smac_m$	Smac/Diablo inside the mitochondria, in MC
$Smac_r$	Smac/Diablo released from the mitochondria, but remaining in the MC
$Smac$	Smac/Diablo in the CC
$Apaf$	Apoptosis Activating Factor (Apaf-1), substrate of CyC, inactive form
$Apaf^*$	active form of Apaf-1
$C9$	inactive form of procaspase-9
$Apop$	the apoptosome, which is the complex $Apaf^* : C9$
$C3^*_{Ub}$	$C3^*$ ubiquinated and targeted for degradation, assumed inactive

Table S2. EARM v1.0 Biochemical Equations

Reaction

$$L + R \underset{k_{-1}}{\overset{k_1}{\rightleftharpoons}} L:R \xrightarrow{\kappa_1} R^*$$

$$R^* + flip \underset{k_{-2}}{\overset{k_2}{\rightleftharpoons}} R^*:flip$$

$$R^* + C8 \underset{k_{-3}}{\overset{k_3}{\rightleftharpoons}} R^*:C8 \xrightarrow{\kappa_3} R^* + C8^*$$

$$C8^* + Bar \underset{k_{-4}}{\overset{k_4}{\rightleftharpoons}} C8^*:Bar$$

$$C8^* + C3 \underset{k_{-5}}{\overset{k_5}{\rightleftharpoons}} C8^*:C3 \xrightarrow{\kappa_5} C8^* + C3^*$$

$$C3^* + C6 \underset{k_{-6}}{\overset{k_6}{\rightleftharpoons}} C3^*:C6 \xrightarrow{\kappa_6} C3^* + C6^*$$

$$C6^* + C8 \underset{k_{-7}}{\overset{k_7}{\rightleftharpoons}} C6^*:C8 \xrightarrow{\kappa_7} C6^* + C8^*$$

$$C3^* + XIAP \underset{k_{-8}}{\overset{k_8}{\rightleftharpoons}} C3^*:XIAP \xrightarrow{\kappa_8} C3^*_{Ub} + XIAP$$

$$C3^* + PARP \underset{k_{-9}}{\overset{k_9}{\rightleftharpoons}} C3^*:PARP \xrightarrow{\kappa_9} C3^* + cPARP$$

$$C8^* + Bid \underset{k_{-10}}{\overset{k_{10}}{\rightleftharpoons}} C8^*:Bid \xrightarrow{\kappa_{10}} C8^* + tBid$$

$$Bid + Bcl2_c \underset{k_{-11}}{\overset{k_{11}}{\rightleftharpoons}} Bid:Bcl2_c$$

$$tBid + Bax \underset{k_{-12}}{\overset{k_{12}}{\rightleftharpoons}} tBid:Bax \xrightarrow{\kappa_{12}} tBid + Bax^*$$

$$Bax^* \underset{k_{-13}}{\overset{k_{13}}{\rightleftharpoons}} Bax^*_m$$

$$Bax^*_m + Bcl2 \underset{k_{-14}}{\overset{k_{14}}{\rightleftharpoons}} Bax^*_m:Bcl2$$

$$Bax^*_m + Bax^*_m \underset{k_{-15}}{\overset{k_{15}}{\rightleftharpoons}} Bax_2$$

$$Bax_2 + Bcl2 \underset{k_{-16}}{\overset{k_{16}}{\rightleftharpoons}} Bax_2:Bcl2$$

$$Bax_2 + Bax_2 \underset{k_{-17}}{\overset{k_{17}}{\rightleftharpoons}} Bax_4$$

$$Bax_4 + Bcl2 \underset{k_{-18}}{\overset{k_{18}}{\rightleftharpoons}} Bax_4:Bcl2$$

$$Bax_4 + M \underset{k_{-19}}{\overset{k_{19}}{\rightleftharpoons}} Bax_4:M \xrightarrow{\kappa_{19}} M^*$$

$$M^* + CyC_m \underset{k_{-20}}{\overset{k_{20}}{\rightleftharpoons}} M^*:CyC_m \xrightarrow{\kappa_{20}} M^* + CyC_r$$

$$M^* + Smac_m \underset{k_{-21}}{\overset{k_{21}}{\rightleftharpoons}} M^*:Smac_m \xrightarrow{\kappa_{21}} M^* + Smac_r$$

$$CyC_r \underset{k_{-22}}{\overset{k_{22}}{\rightleftharpoons}} CyC$$

$$CyC + Apaf \underset{k_{-23}}{\overset{k_{23}}{\rightleftharpoons}} CyC:Apaf \xrightarrow{\kappa_{23}} CyC + Apaf^*$$

$$Apaf^* + C9 \underset{k_{-24}}{\overset{k_{24}}{\rightleftharpoons}} Apop$$

$$Apop + C3 \underset{k_{-25}}{\overset{k_{25}}{\rightleftharpoons}} Apop:C3 \xrightarrow{\kappa_{25}} Apop + C3^*$$

$$Smac_r \underset{k_{-26}}{\overset{k_{26}}{\rightleftharpoons}} Smac$$

$$Apop + XIAP \underset{k_{-27}}{\overset{k_{27}}{\rightleftharpoons}} Apop:XIAP$$

$$Smac + XIAP \underset{k_{-28}}{\overset{k_{28}}{\rightleftharpoons}} Smac:XIAP$$

Table S3. EARM v1.0 Rate Constant Values

i	k_i ((#/CC)$^{-1}$·sec^{-1})	k_i ((M)$^{-1}$·sec^{-1})	k_{-i} (sec^{-1})	κ_i (sec^{-1})
1	4×10^{-7}	2.4×10^{5}	10^{-3}	10^{-5}
2	10^{-6}	6×10^{5}	10^{-3}	
3	10^{-6}	6×10^{5}	10^{-3}	1
4	10^{-6}	6×10^{5}	10^{-3}	
5	10^{-7}	6×10^{4}	10^{-3}	1
6	10^{-6}	6×10^{5}	10^{-3}	1
7	3×10^{-8}	1.8×10^{4}	10^{-3}	1
8	2×10^{-6}	1.2×10^{6}	10^{-3}	0.1
9	10^{-6}	6×10^{5}	10^{-2}	1
10	10^{-7}	6×10^{4}	10^{-3}	1
11	10^{-6}	6×10^{5}	10^{-3}	
12	10^{-7}	6×10^{4}	10^{-3}	1
13	10^{-2} (sec^{-1})		10^{-2}	
14	10^{-6} ((#/MC)$^{-1}$·sec^{-1})	6×10^{5}	10^{-3}	
15	10^{-6} ((#/MC)$^{-1}$·sec^{-1})	6×10^{5}	10^{-3}	
16	10^{-6} ((#/MC)$^{-1}$·sec^{-1})	6×10^{5}	10^{-3}	
17	10^{-6} ((#/MC)$^{-1}$·sec^{-1})	6×10^{5}	10^{-3}	
18	10^{-6} ((#/MC)$^{-1}$·sec^{-1})	6×10^{5}	10^{-3}	
19	10^{-6} ((#/MC)$^{-1}$·sec^{-1})	6×10^{5}	10^{-3}	1
20	2×10^{-6} ((#/MC)$^{-1}$·sec^{-1})	1.2×10^{6}	10^{-3}	10
21	2×10^{-6} ((#/MC)$^{-1}$·sec^{-1})	1.2×10^{6}	10^{-3}	10
22	10^{-2} (sec^{-1})		10^{-2}	
23	5×10^{-7}	3×10^{5}	10^{-3}	1
24	5×10^{-8}	3×10^{4}	10^{-3}	
25	5×10^{-9}	3×10^{3}	10^{-3}	1
26	10^{-2} (sec^{-1})		10^{-2}	
27	2×10^{-6}	1.2×10^{6}	10^{-3}	
28	7×10^{-6}	4.2×10^{6}	10^{-3}	

Table S4. References for Rate Constants

Enzymatic Reaction	Km (#/cell) or (M)	k_{cat} (sec^{-1})	k_{cat}/Km (cell/#/sec) or (1/M/sec)	Ref	substrate
*C8**					
Garcia-Calvo *et.al.* 1999	$4.2 \times 10^7 / 7.0 \times 10^{-5}$	0.37	$8.8 \times 10^{-9} / 5300$	(1)	LETD
Stennicke *et.al.* 1998			$1.5 \times 10^{-6} / 9.0 \times 10^5$	(2)	caspase-3
Stennicke *et.al.* 2000	$1.1 \times 10^7 / 1.8 \times 10^{-5}$	0.69	$6.4 \times 10^{-8} / 3.8 \times 10^4$	(3)	DEVDG
*C3**					
Bose *et.al.* 2003	$1.3 \times 10^6 / 2.2 \times 10^{-6}$	0.4	$3.0 \times 10^{-7} / 1.8 \times 10^5$	(4)	DEVD
Casciola-Rosen *et.al.* 1996			$8.6 \times 10^{-6} / 5.2 \times 10^6$	(5)	PARP
Casciola-Rosen *et.al.* 1996			$1.2 \times 10^{-5} / 7.2 \times 10^6$	(5)	DNA-PK
Casciola-Rosen *et.al.* 1996			$3.8 \times 10^{-6} / 2.3 \times 10^6$	(5)	UI-70K
Garcia-Calvo *et.al.* 1999	$6.0 \times 10^6 / 1.0 \times 10^{-5}$	14	$2.3 \times 10^{-6} / 1.4 \times 10^6$	(1)	DEVD
Margolin *et.al.* 1997	$6.0 \times 10^6 / 1.0 \times 10^{-5}$	23	$3.8 \times 10^{-6} / 2.3 \times 10^6$	(6)	PARP
Stennicke *et.al.* 2000	$7.8 \times 10^6 / 1.3 \times 10^{-5}$	2.5	$3.2 \times 10^{-7} / 1.9 \times 10^5$	(3)	DEVDG
Talanian *et.al.* 1997	$6.6 \times 10^6 / 1.1 \times 10^{-5}$	2.4	$3.6 \times 10^{-7} / 2.2 \times 10^5$	(7)	DEVD
*C6**					
Garcia-Calvo *et.al.* 1999	$1.0 \times 10^8 / 1.7 \times 10^{-4}$			(1)	VEHD
C9					
Garcia-Calvo *et.al.* 1999	$4.7 \times 10^8 / 7.8 \times 10^{-4}$	0.1	$2.6 \times 10^{-10} / 160$	(1)	LEHD
Talanian *et.al.* 1997	$1.8 \times 10^7 / 3.0 \times 10^{-5}$	5	$2.7 \times 10^{-7} / 1.6 \times 10^5$	(7)	VEID

Binding Reaction	k_{on} $((\#/cell)^{-1} \cdot sec^{-1})$ or $(M^{-1} \cdot sec^{-1})$	k_{off} (sec^{-1})	Kd (#/cell) or (M)	Ref	protein fragments
XIAP : C3/7**					
Huang *et.al* 2003	$3.5 \times 10^{-6} / 2.1 \times 10^6$	0.0021	$600 / 1 \times 10^{-9}$	(8)	caspase-7/linkerBIR2
Riedl *et.al* 2001	$4.2 \times 10^{-6} / 2.5 \times 10^6$	0.0024	$570 / 9.6 \times 10^{-10}$	(9)	caspase-3/BIR2
Riedl *et.al* 2001	$2.3 \times 10^{-5} / 1.4 \times 10^7$	0.0014	$61 / 1 \times 10^{-10}$	(9)	caspase-7/BIR2
XIAP : Casp9					
Sun *et.al* 2000			$6700 / 1.1 \times 10^{-8}$	(10)	BIR2-RF(aa 241-497) of XIAP
Smac : XIAP					
Hung *et.al* 2003	$1.2 \times 10^{-5} / 7.2 \times 10^6$	0.0022	$180 / 3 \times 10^{-10}$	(8)	Smac/linker_BIR2_BIR3

Table S5. Variable Definitions and Initial Conditions for EARM v1.0

variable	state	model IC (#/CC) or (M)	ref
x_1	$[L]$	$3 \times 10^3/5.1 \times 10^{-9} = 50$ ng/ml	
x_2	$[R]$ WT	$2 \times 10^2/3.4 \times 10^{-10}$	
	$[R]$ siRNA-treated	$10^5/1.7 \times 10^{-7}$	
x_3	$[L:R]$	0	
x_4	$[R^*]$	0	
x_5	$[flip]$	$10^2/1.7 \times 10^{-10}$	
x_6	$[flip:R^*]$	0	
x_7	$[C8]$	$2 \times 10^4/3.4 \times 10^{-8}$	(1)
x_8	$[C8:R^*]$	0	
x_9	$[C8^*]$	0	
x_{10}	$[Bar]$	$10^3/1.7 \times 10^{-9}$	
x_{11}	$[C8^*:Bar]$	0	
x_{12}	$[C3]$	$10^4/1.7 \times 10^{-8}$	(1,2 ,3)
x_{13}	$[C8^*:C3]$	0	
x_{14}	$[C3^*]$	0	
x_{15}	$[C6]$	$10^4/1.7 \times 10^{-8}$	
x_{16}	$[C3^*:C6]$	0	
x_{17}	$[C6^*]$	0	
x_{18}	$[C6^*:C8]$	0	
x_{19}	$[XIAP]$	$10^5/1.7 \times 10^{-7}$	(3)
x_{20}	$[XIAP:C3^*]$	0	
x_{21}	$[PARP]$	$10^6/1.7 \times 10^{-6}$	
x_{22}	$[C3^*:PARP]$	0	
x_{23}	$[cPARP]$	0	
x_{24}	$[Bid]$	4×10^4	
x_{25}	$[C8^*:Bid]$	0	
x_{26}	$[tBid]$	0	
x_{27}	$[Bcl2_c]$	$2 \times 10^4/3.4 \times 10^{-8}$	
x_{28}	$[tBid:Bcl2_c]$	0	
x_{29}	$[Bax]$	$10^5/1.7 \times 10^{-7}$	
x_{30}	$[tBid:Bax]$	0	
x_{31}	$[Bax^*]$	0	
x_{32}	$[Bax^*_m]$	0 (#/MC)	
x_{33}	$[Bcl2]$	2×10^4 (#/MC)/4.8×10^{-7}	
x_{34}	$[Bax^*_m:Bcl2]$	0 (#/MC)	
x_{35}	$[Bax_2]$	0 (#/MC)	
x_{36}	$[Bax_2:Bcl2]$	0 (#/MC)	
x_{37}	$[Bax_4]$	0 (#/MC)	
x_{38}	$[Bax_4:Bcl2]$	0 (#/MC)	
x_{39}	$[M]$	5×10^5 (#/MC)/1.2×10^{-5}	
x_{40}	$[Bax_4:M]$	0 (#/MC)	
x_{41}	$[M^*]$	0 (#/MC)	
x_{42}	$[CyC_m]$	5×10^5 (#/MC)/1.2×10^{-5}	(4)
x_{43}	$[M^*:CyC_m]$	0 (#/MC)	
x_{44}	$[CyC_r]$	0 (#/MC)	
x_{45}	$[Smac_m]$	10^5 (#/MC)/2.4×10^{-6}	
x_{46}	$[M^*:Smac_m]$	0 (#/MC)	
x_{47}	$[Smac_r]$	0 (#/MC)	
x_{48}	$[CyC]$	0	
x_{49}	$[Apaf]$	$10^5/1.7 \times 10^{-7}$	(3)
x_{50}	$[Apaf:CyC]$	0	
x_{51}	$[Apaf^*]$	0	
x_{52}	$[C9]$	$10^5/1.7 \times 10^{-7}$	(3)
x_{53}	$[Apop]$	0	
x_{54}	$[Apop:C3]$	0	
x_{55}	$[Smac]$	0	
x_{56}	$[Apop:XIAP]$	0	
x_{57}	$[Smac:XIAP]$	0	
x_{58}	$[C3^*_{Ub}]$	0	

Table S6. EARM v1.0 Equations

$$
\begin{aligned}
\dot{x}_1 &= -k_1x_1x_2 + k_{-1}x_3 \\
\dot{x}_2 &= -k_1x_1x_2 + k_{-1}x_3 \\
\dot{x}_3 &= k_1x_1x_2 - k_{-1}x_3 - \kappa_1x_3 \\
\dot{x}_4 &= \kappa_1x_3 - k_2x_4x_5 + k_{-2}x_6 + ... \\
&\quad -k_3x_4x_7 + k_{-3}x_8 + \kappa_3x_8 \\
\dot{x}_5 &= -k_2x_4x_5 + k_{-2}x_6 \\
\dot{x}_6 &= k_2x_4x_5 - k_{-2}x_6 \\
\dot{x}_7 &= -k_3x_4x_7 + k_{-3}x_8 + ... \\
&\quad -k_7x_7x_{17} + k_{-7}x_{18} \\
\dot{x}_8 &= k_3x_4x_7 - k_{-3}x_8 - \kappa_3x_8 \\
\dot{x}_9 &= \kappa_3x_8 - k_4x_9x_{10} + k_{-4}x_{11} + ... \\
&\quad -k_5x_9x_{12} + k_{-5}x_{13} + \kappa_5x_{13} + ... \\
&\quad +\kappa_7x_{18} + ... \\
&\quad -k_{10}x_9x_{24} + k_{-10}x_{25} + \kappa_{10}x_{25} \\
\dot{x}_{10} &= -k_4x_9x_{10} + k_{-4}x_{11} \\
\dot{x}_{11} &= k_4x_9x_{10} - k_{-4}x_{11} \\
\dot{x}_{12} &= -k_5x_9x_{12} + k_{-5}x_{13} + ... \\
&\quad -k_{25}x_{12}x_{53} + k_{-25}x_{54} \\
\dot{x}_{13} &= k_5x_9x_{12} - k_{-5}x_{13} - \kappa_5x_{13} \\
\dot{x}_{14} &= \kappa_5x_{13} + \kappa_{25}x_{54} + ... \\
&\quad -k_6x_{14}x_{15} + k_{-6}x_{16} + \kappa_6x_{16} + ... \\
&\quad -k_8x_{14}x_{19} + k_{-8}x_{20} + ... \\
&\quad -k_9x_{14}x_{21} + k_{-9}x_{22} + \kappa_9x_{22} \\
\dot{x}_{15} &= -k_6x_{14}x_{15} + k_{-6}x_{16} \\
\dot{x}_{16} &= k_6x_{14}x_{15} - k_{-6}x_{16} - \kappa_6x_{16}
\end{aligned}
$$

$$
\begin{aligned}
\dot{x}_{33} &= -\frac{1}{v}k_{14}x_{32}x_{33} + k_{-14}x_{34} + ... \\
&\quad -\frac{1}{v}k_{16}x_{33}x_{35} + k_{-16}x_{36} + ... \\
&\quad -\frac{1}{v}k_{18}x_{33}x_{37} + k_{-18}x_{38} \\
\dot{x}_{34} &= \frac{1}{v}k_{14}x_{32}x_{33} - k_{-14}x_{34} \\
\dot{x}_{35} &= \frac{1}{v}k_{15}x_{32}^2 - k_{-15}x_{35} + ... \\
&\quad -\frac{1}{v}k_{16}x_{33}x_{35} + k_{-16}x_{36} + ... \\
&\quad -\frac{2}{v}k_{17}x_{35}^2 + 2k_{-17}x_{37} \\
\dot{x}_{36} &= \frac{1}{v}k_{16}x_{33}x_{35} - k_{-16}x_{36} \\
\dot{x}_{37} &= \frac{1}{v}k_{17}x_{35}^2 - k_{-17}x_{37} + ... \\
&\quad -\frac{1}{v}k_{18}x_{33}x_{37} + k_{-18}x_{38} + ... \\
&\quad -\frac{1}{v}k_{19}x_{39}x_{37} + k_{-19}x_{40} \\
\dot{x}_{38} &= \frac{1}{v}k_{18}x_{33}x_{37} - k_{-18}x_{38} \\
\dot{x}_{39} &= -\frac{1}{v}k_{19}x_{39}x_{37} + k_{-19}x_{40} \\
\dot{x}_{40} &= \frac{1}{v}k_{19}x_{39}x_{37} - k_{-19}x_{40} - \kappa_{19}x_{40} \\
\dot{x}_{41} &= \kappa_{19}x_{40} + ... \\
&\quad -\frac{1}{v}k_{20}x_{41}x_{42} + k_{-20}x_{43} + \kappa_{20}x_{43} + ... \\
&\quad -\frac{1}{v}k_{21}x_{41}x_{45} + k_{-21}x_{46} + \kappa_{21}x_{46}
\end{aligned}
$$

$$
\begin{aligned}
\dot{x}_{17} &= \kappa_6x_{16} + ... \\
&\quad -k_7x_7x_{17} + k_{-7}x_{18} + \kappa_7x_{18} \\
\dot{x}_{18} &= k_7x_7x_{17} - k_{-7}x_{18} - \kappa_7x_{18} \\
\dot{x}_{19} &= -k_8x_{14}x_{19} + k_{-8}x_{20} + \kappa_8x_{20} + ... \\
&\quad -k_{27}x_{19}x_{53} + k_{-27}x_{56} + ... \\
&\quad -k_{28}x_{19}x_{55} + k_{-28}x_{57} \\
\dot{x}_{20} &= k_8x_{14}x_{19} - k_{-8}x_{20} - \kappa_8x_{20} \\
\dot{x}_{21} &= -k_9x_{14}x_{21} + k_{-9}x_{22} \\
\dot{x}_{22} &= k_9x_{14}x_{21} - k_{-9}x_{22} - \kappa_9x_{22} \\
\dot{x}_{23} &= \kappa_9x_{22} \\
\dot{x}_{24} &= -k_{10}x_9x_{24} + k_{-10}x_{25} \\
\dot{x}_{25} &= k_{10}x_9x_{24} - k_{-10}x_{25} - \kappa_{10}x_{25} \\
\dot{x}_{26} &= \kappa_{10}x_{25} - k_{11}x_{26}x_{27} + k_{-11}x_{28} + ... \\
&\quad -k_{12}x_{26}x_{29} + k_{-12}x_{30} + \kappa_{12}x_{30} \\
\dot{x}_{27} &= -k_{11}x_{26}x_{27} + k_{-11}x_{28} \\
\dot{x}_{28} &= k_{11}x_{26}x_{27} - k_{-11}x_{28} \\
\dot{x}_{29} &= -k_{12}x_{26}x_{29} + k_{-12}x_{30} \\
\dot{x}_{30} &= k_{12}x_{26}x_{29} - k_{-12}x_{30} - \kappa_{12}x_{30} \\
\dot{x}_{31} &= \kappa_{12}x_{30} - k_{13}x_{31} + k_{-13}x_{32} \\
\dot{x}_{32} &= k_{13}x_{31} - k_{-13}x_{32} + ... \\
&\quad -\frac{1}{v}k_{14}x_{32}x_{33} + k_{-14}x_{34} + ... \\
&\quad -\frac{2}{v}k_{15}x_{32}^2 + 2k_{-15}x_{35}
\end{aligned}
$$

$$
\begin{aligned}
\dot{x}_{42} &= -\frac{1}{v}k_{20}x_{41}x_{42} + k_{-20}x_{43} \\
\dot{x}_{43} &= \frac{1}{v}k_{20}x_{41}x_{42} - k_{-20}x_{43} - \kappa_{20}x_{43} \\
\dot{x}_{44} &= \kappa_{20}x_{43} - k_{22}x_{44} + k_{-22}x_{48} \\
\dot{x}_{45} &= -\frac{1}{v}k_{21}x_{41}x_{45} + k_{-21}x_{46} \\
\dot{x}_{46} &= \frac{1}{v}k_{21}x_{41}x_{45} - k_{-21}x_{46} - \kappa_{21}x_{46} \\
\dot{x}_{47} &= \kappa_{21}x_{46} - k_{26}x_{47} + k_{-26}x_{55} \\
\dot{x}_{48} &= k_{22}x_{44} - k_{-22}x_{48} + ... \\
&\quad -k_{23}x_{48}x_{49} + k_{-23}x_{50} + \kappa_{23}x_{50} \\
\dot{x}_{49} &= -k_{23}x_{48}x_{49} + k_{-23}x_{50} \\
\dot{x}_{50} &= k_{23}x_{48}x_{49} - k_{-23}x_{50} - \kappa_{23}x_{50} \\
\dot{x}_{51} &= \kappa_{23}x_{50} - k_{24}x_{51}x_{52} + k_{-24}x_{53} \\
\dot{x}_{52} &= -k_{24}x_{51}x_{52} + k_{-24}x_{53} \\
\dot{x}_{53} &= k_{24}x_{51}x_{52} - k_{-24}x_{53} + ... \\
&\quad -k_{25}x_{12}x_{53} + k_{-25}x_{54} + \kappa_{25}x_{54} + ... \\
&\quad -k_{27}x_{19}x_{53} + k_{-27}x_{56} \\
\dot{x}_{54} &= k_{25}x_{12}x_{53} - k_{-25}x_{54} - \kappa_{25}x_{54} \\
\dot{x}_{55} &= k_{26}x_{47} - k_{-26}x_{55} + ... \\
&\quad -k_{28}x_{19}x_{55} + k_{-28}x_{57} \\
\dot{x}_{56} &= k_{27}x_{19}x_{53} - k_{-27}x_{56} \\
\dot{x}_{57} &= k_{28}x_{19}x_{55} - k_{-28}x_{57} \\
\dot{x}_{58} &= \kappa_8x_{20}
\end{aligned}
$$

2. Experimental Determination of C3 Activation Dynamics

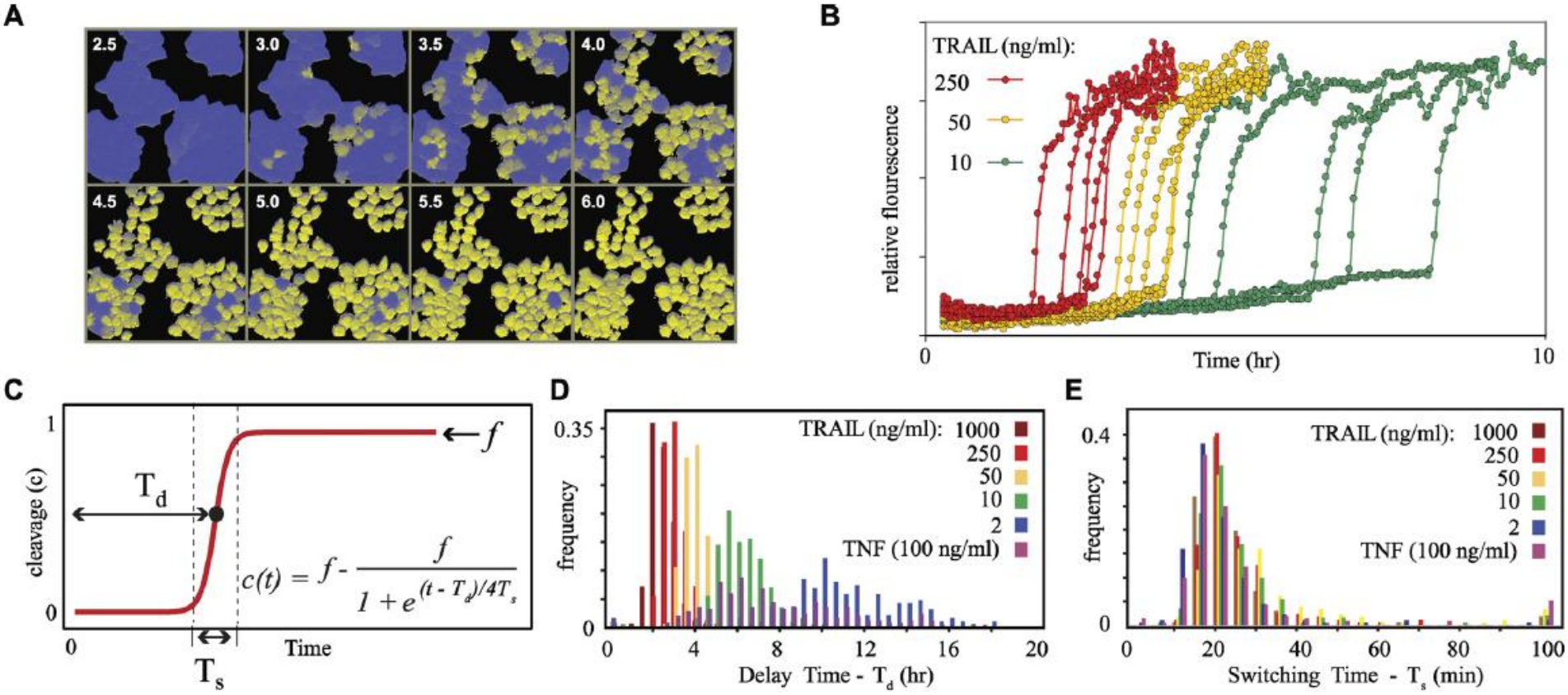

Figure 2. Dynamics of Caspase Activation in Cells Treated with TNF or TRAIL

(A) Time-lapse images of HeLa cells expressing EC-RP; cleavage of EC-RP caused a shift in the 465/535 ratio that was pseudo-colored as a shift from blue to yellow.

(B) Time courses of EC-RP cleavage in individual HeLa cells.

(C) Idealized single-cell time course for EC-RP cleavage, showing relationships among Td (delay time), Ts (switch time), and f (fraction substrate cleaved).

(D, E) Frequency distributions for Td (D) and Ts (E) determined by live-cell microscopy in EC-RP-expressing HeLa cells (n > 100 for each condition);

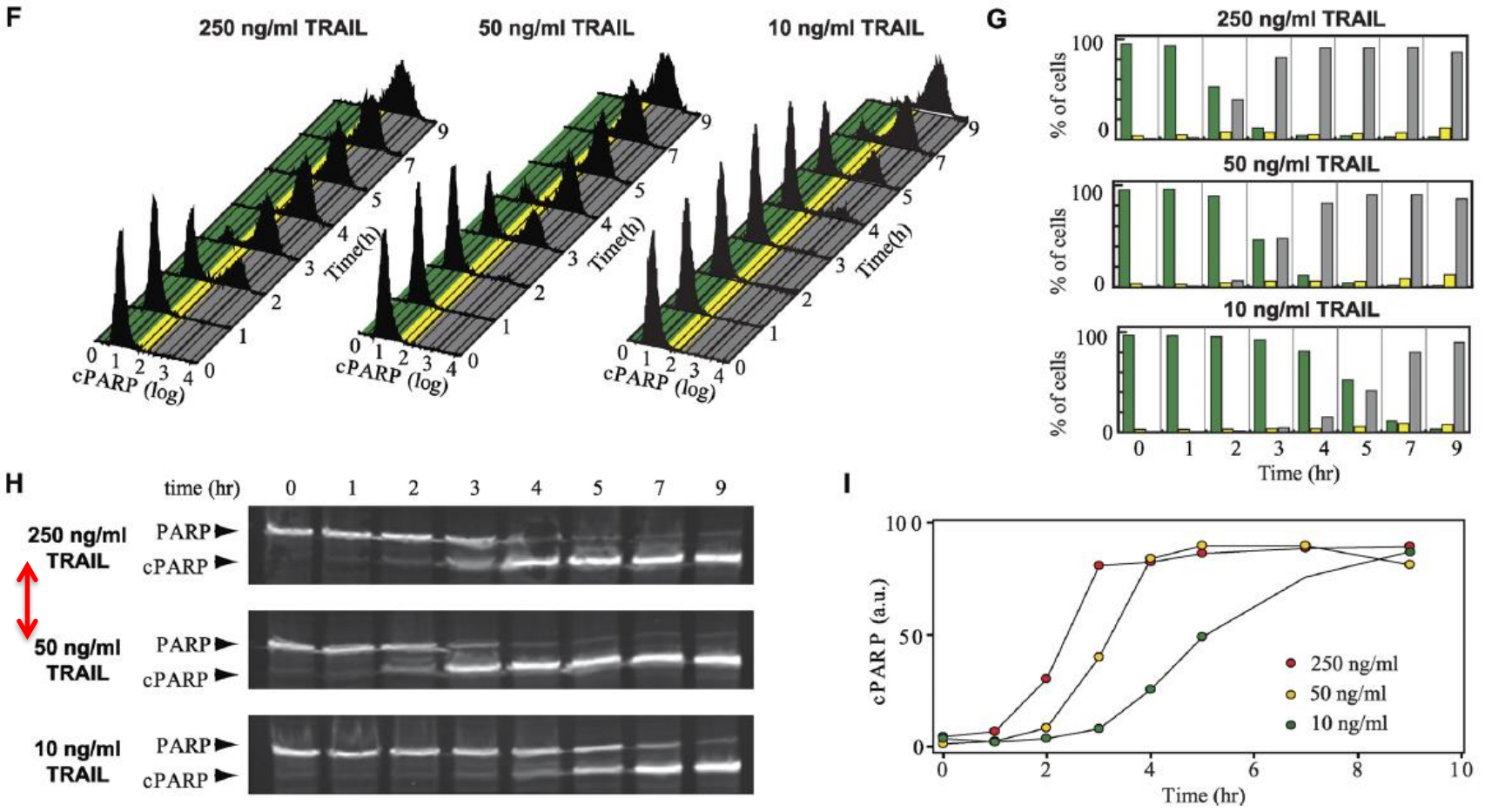

Figure 2. Dynamics of Caspase Activation in Cells Treated with TNF or TRAIL
(F) Flow cytometry of PARP cleavage, as assayed with an antibody for PARP cleaved at Asp214 by C3 and C7. (G) Discretized flow cytometry data. The fraction of cells having low, intermediate, or high PARP cleavage is color-coded to match the intervals in (F). (H) Immunoblot analysis of PARP cleavage.
(I) Quantitation of the cleaved 89 kDa form of PARP for blots shown in (H).

Table 1. Values for Switching Parameters Determined by Live-Cell Microscopy

Treatment	Mean T_d (min)	Standard Deviation T_d (min)	Coefficient of Variation T_d (%)	Mean T_s (min)	Standard Deviation T_s (min)
1,000 ng/ml TRAIL	140	32	23	22	9.5
250 ng/ml TRAIL	180	32	18	24	9.5
50 ng/ml TRAIL	240	36	15	27	13
10 ng/ml TRAIL	360	79	22	22	7.7
2 ng/ml TRAIL	660	170	26	19	10
100 ng/ml TNF[a]	460	190	42	22	27

[a]Not all cells committed apoptosis during the experiment under this condition; values reflect only the apoptotic fraction of the population.

doi:10.1371/journal.pbio.0060299.t001

3. Merging Data from Single-Cell and Population-Based Measurements

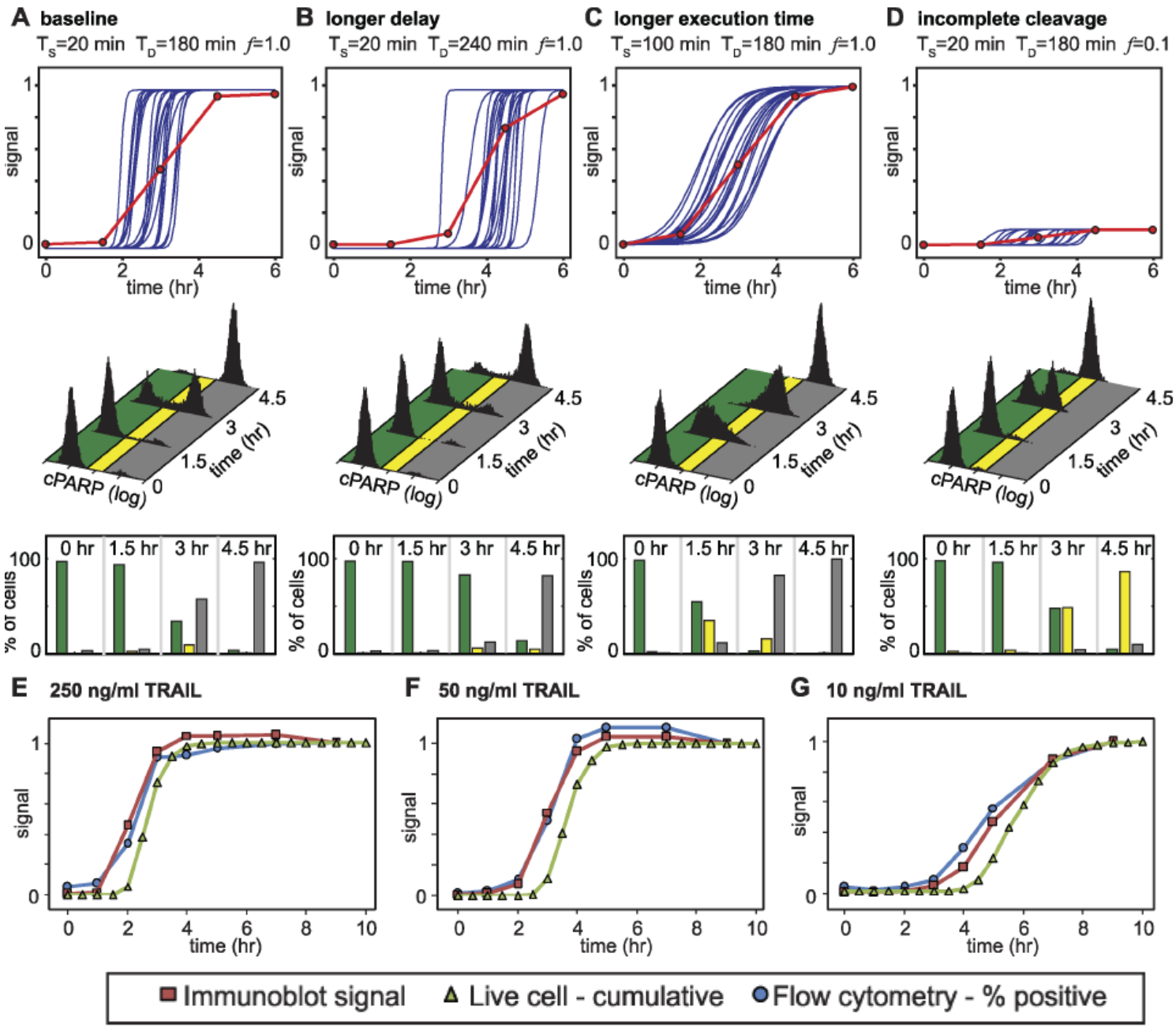

Figure 3. Simulation-Based Approach to Data Fusion for Three Different Measures of Caspase Activity

Table 2. Experimental Determinability of Switching Parameters

Method	T_d (Mean)	T_d (Variance)	T_s (Mean)	T_s (Variance)	*f* (Mean)	*f* (Variance)
Live-cell microscopy	Direct	Direct	Direct	Direct	Inferred	Inferred
Flow cytometry	Direct[a]	Direct[a]	Inferred	Inferred	Inferred	Inferred
Immunoblot	Inferred	Inferred	No	No	Direct	Direct

[a]Assuming irreversible switching.

doi:10.1371/journal.pbio.0060299.t002

4. Linking Models and Experiment Via Perturbation

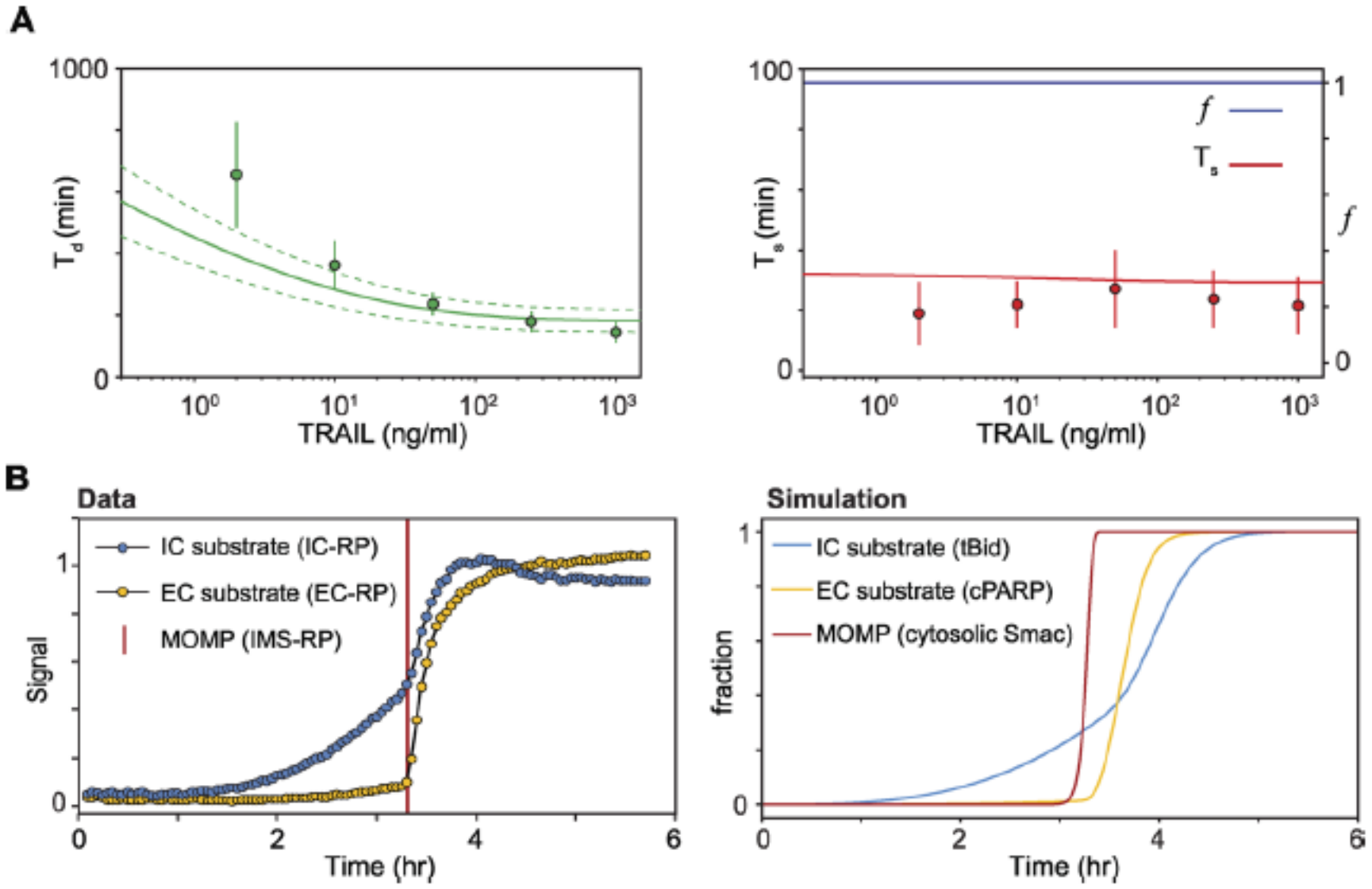

Figure 4. Training Data Derived from Live-Cell Microscopy

(A) Simulation of Td (left) or Ts and f (right) as a function of TRAIL dose (lines) alongside corresponding experimental values.

(B) Composite plot of IC-RP and EC-RP cleavage aligned by the average time of MOMP (left) and model-based simulation of the corresponding species (right).

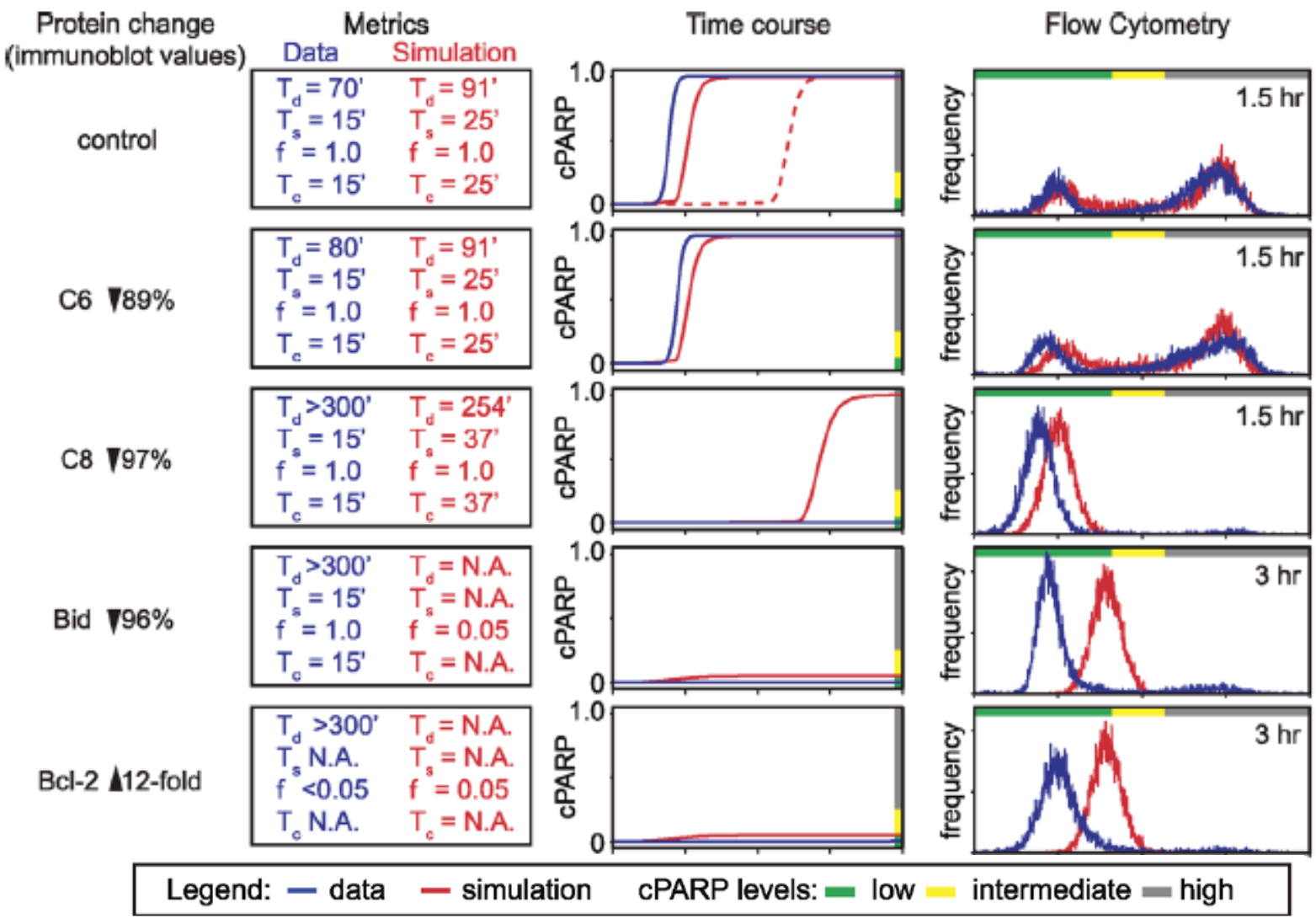

Figure 5. Training the Model on Network-Wide Perturbations

First column: perturbation values measured by immunoblot. Second column: comparison of EARM v1.0-simulated and experimentally derived values for Ts, Td, *f*, and Tc. Third column: comparison of EARM v1.0-simulated cPARP cleavage (red) to time courses derived from flow cytometry using a data model (blue). Fourth column: comparison of experimental (blue) and predicted (red) flow cytometry plots.

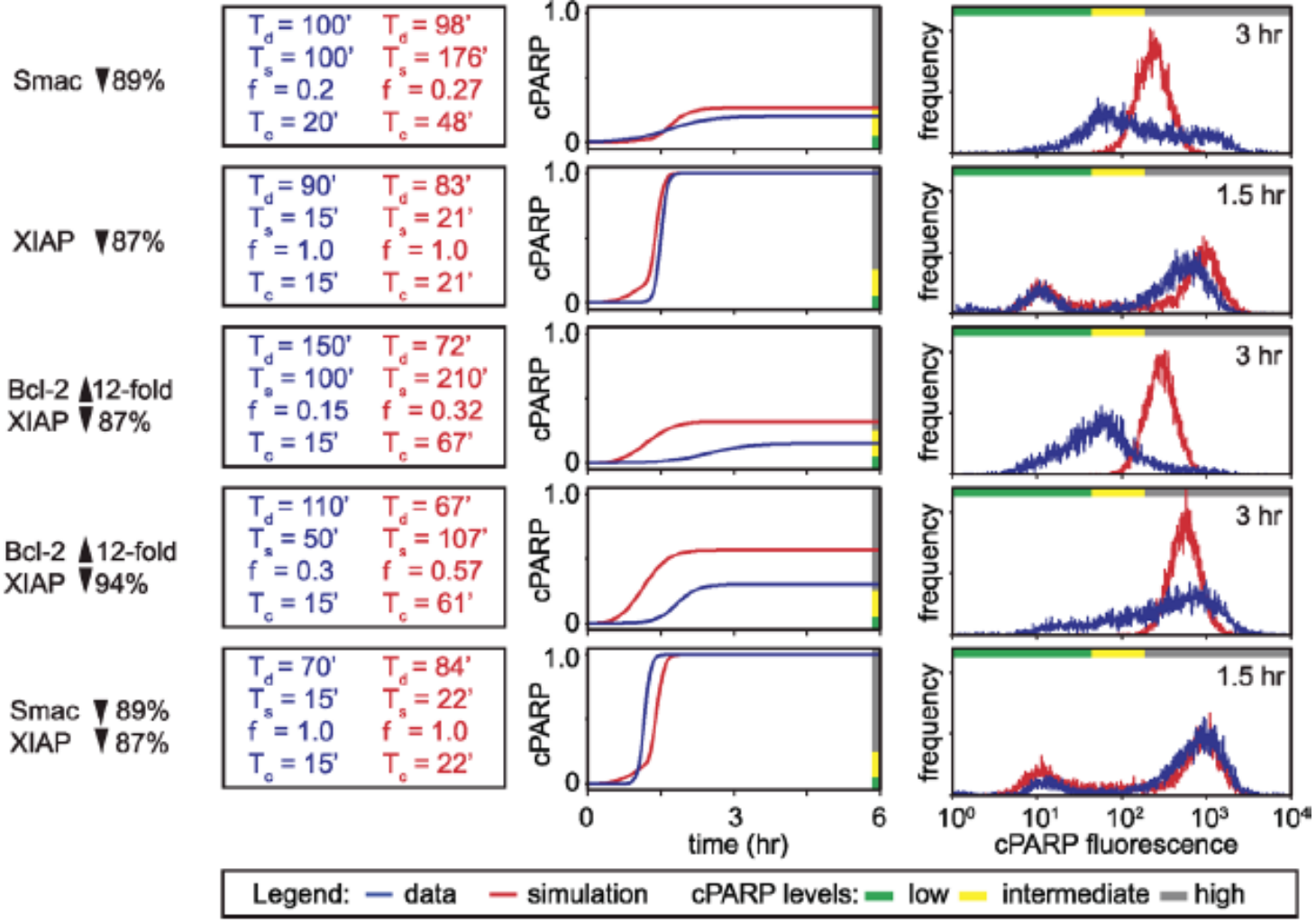

Figure 5. Training the Model on Network-Wide Perturbations
First column: perturbation values measured by immunoblot. Second column: comparison of EARM v1.0-simulated and experimentally derived values for Ts, Td, *f*, and Tc. Third column: comparison of EARM v1.0-simulated cPARP cleavage (red) to time courses derived from flow cytometry using a data model (blue). Fourth column: comparison of experimental (blue) and predicted (red) flow cytometry plots.

5. Transition from a Graded to a Snap-Action Signal

The network

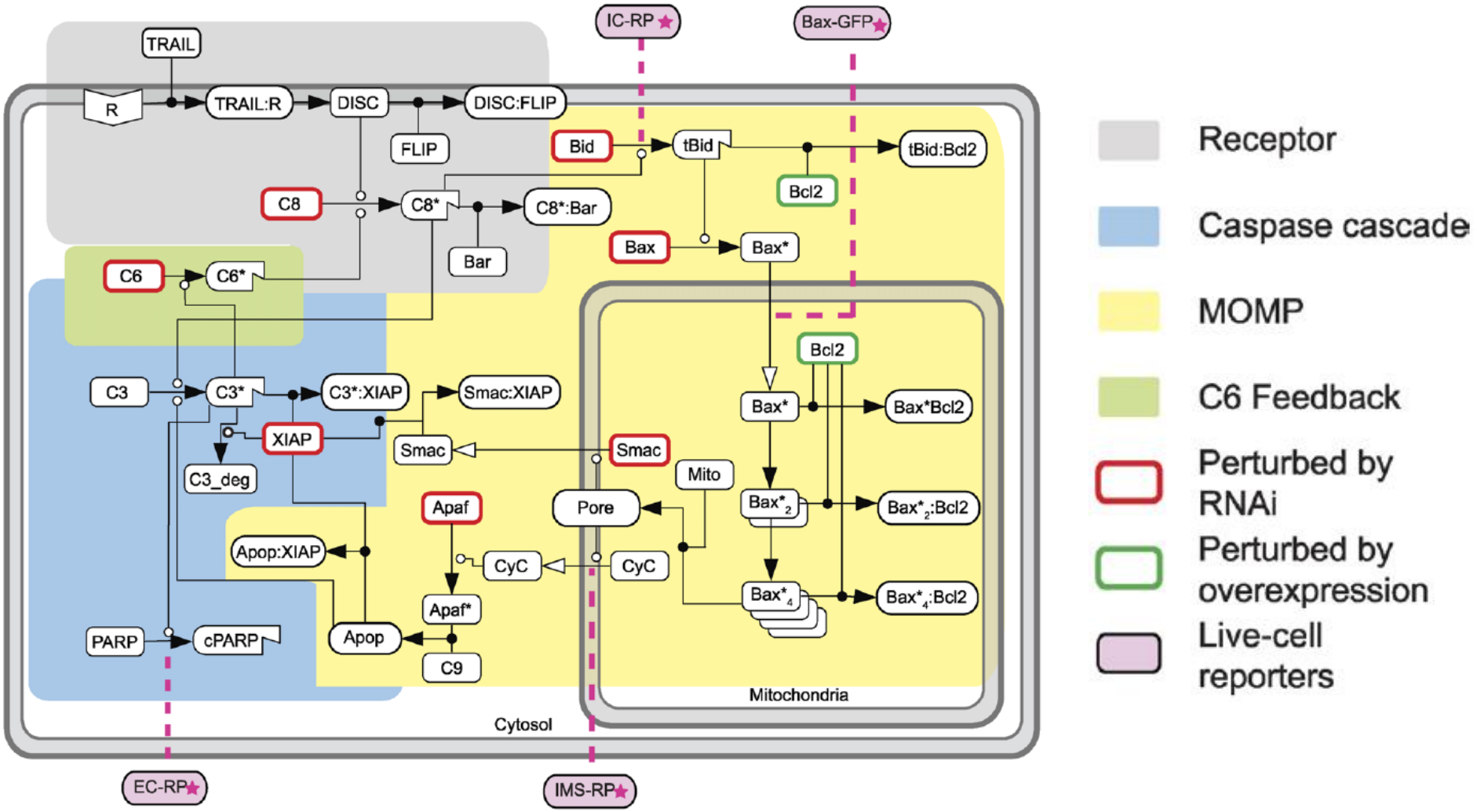

Simplifying: **C8**: C8 and C10; **C3**: C3 and C7;

Bcl-2 family: **Bid**: apoptotic ‘activator’; **Bcl-2**; apoptotic inhibitor

Bax: pore-forming protein

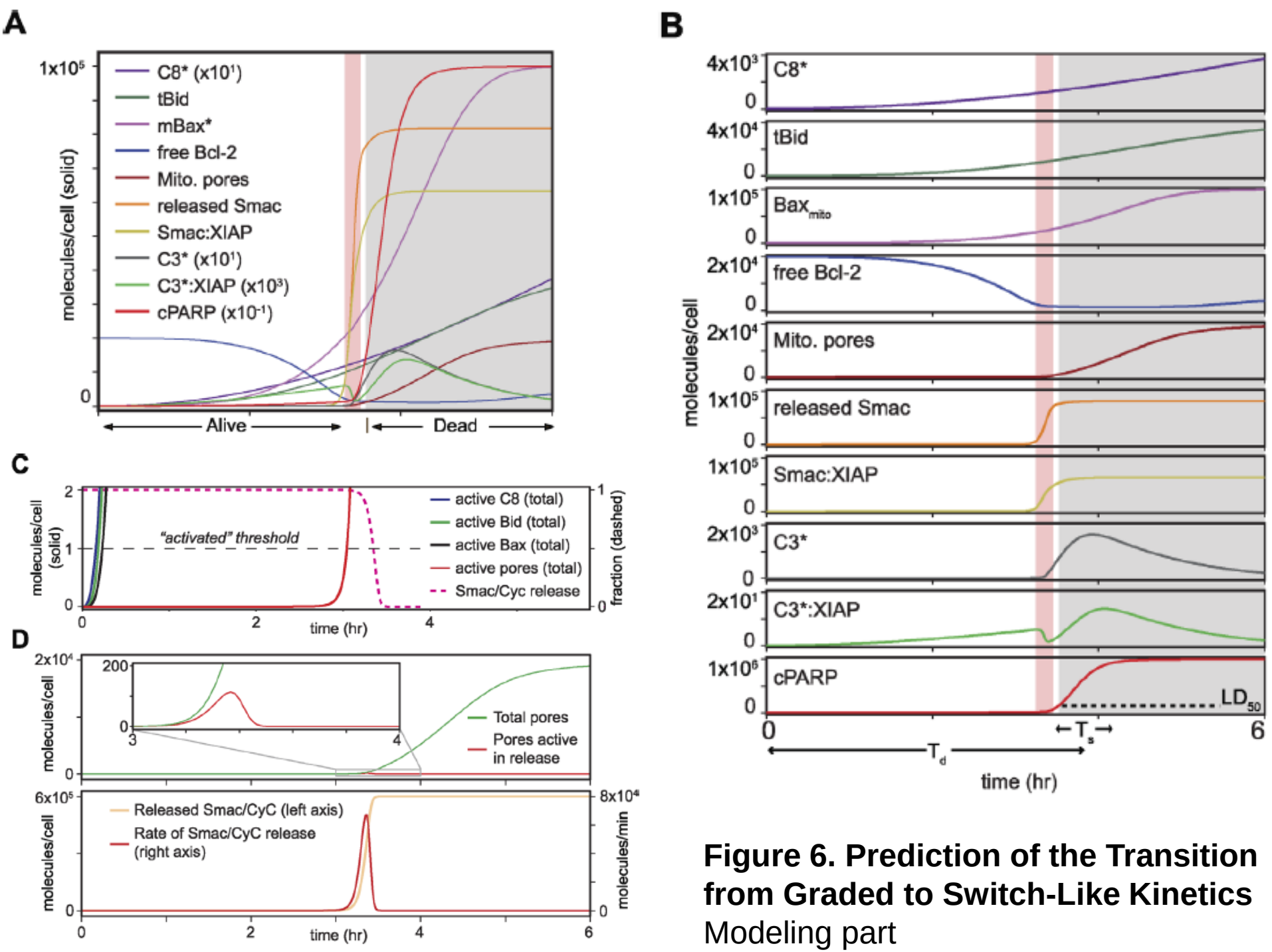

Figure 6. Prediction of the Transition from Graded to Switch-Like Kinetics
Modeling part

6. Predictions I and II:

MOMP Is Complete by the Time Dying Cells Have Assembled Relatively Few Pores

(i) Smac release should begin nearly simultaneously with the formation of the first Bax-containing pores

(ii) Pore formation should continue long after Smac release is complete.

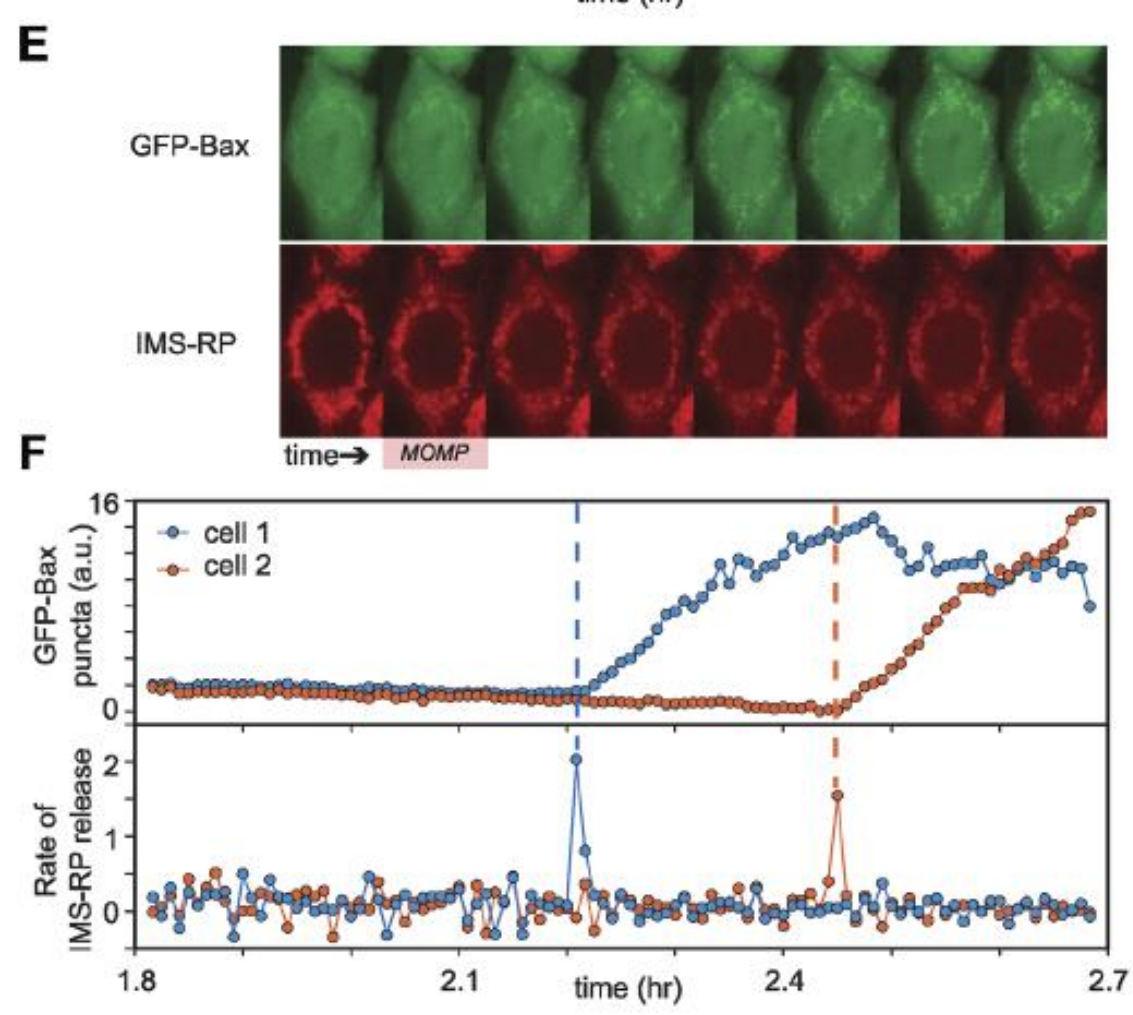

Figure 6. Prediction of the Transition from Graded to Switch-Like Kinetics

Experiments part

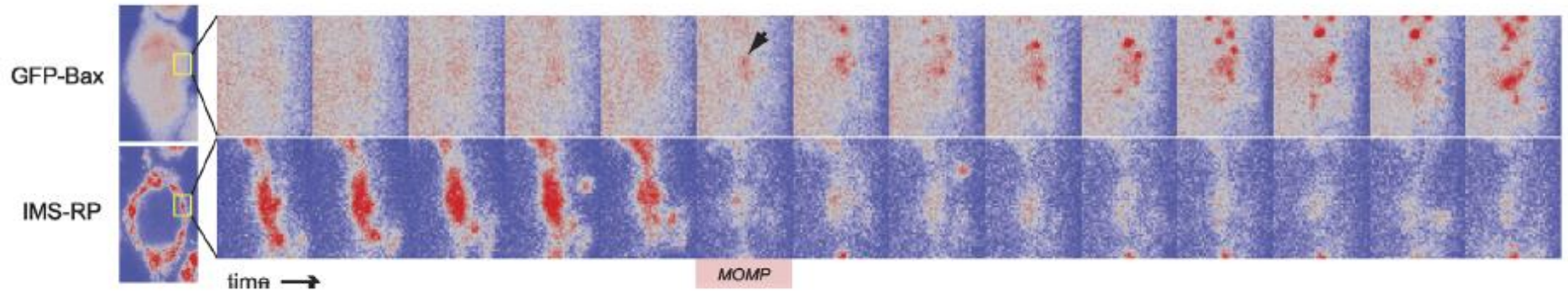

7. Prediction III: Snap-Action Switching Does Not Require Feedback

a. Others shows the rapid post-MOMP phase probably involves feedback processes including (i) cleavage by C3* itself, (ii) cleavage by C8*, whose levels are expected to rise rapidly as a consequence of the C3* → C6* → C8* feedback loop, and (iii) cleavage by C9, an initiator caspase activated by CyC translocation.

Condensed representation

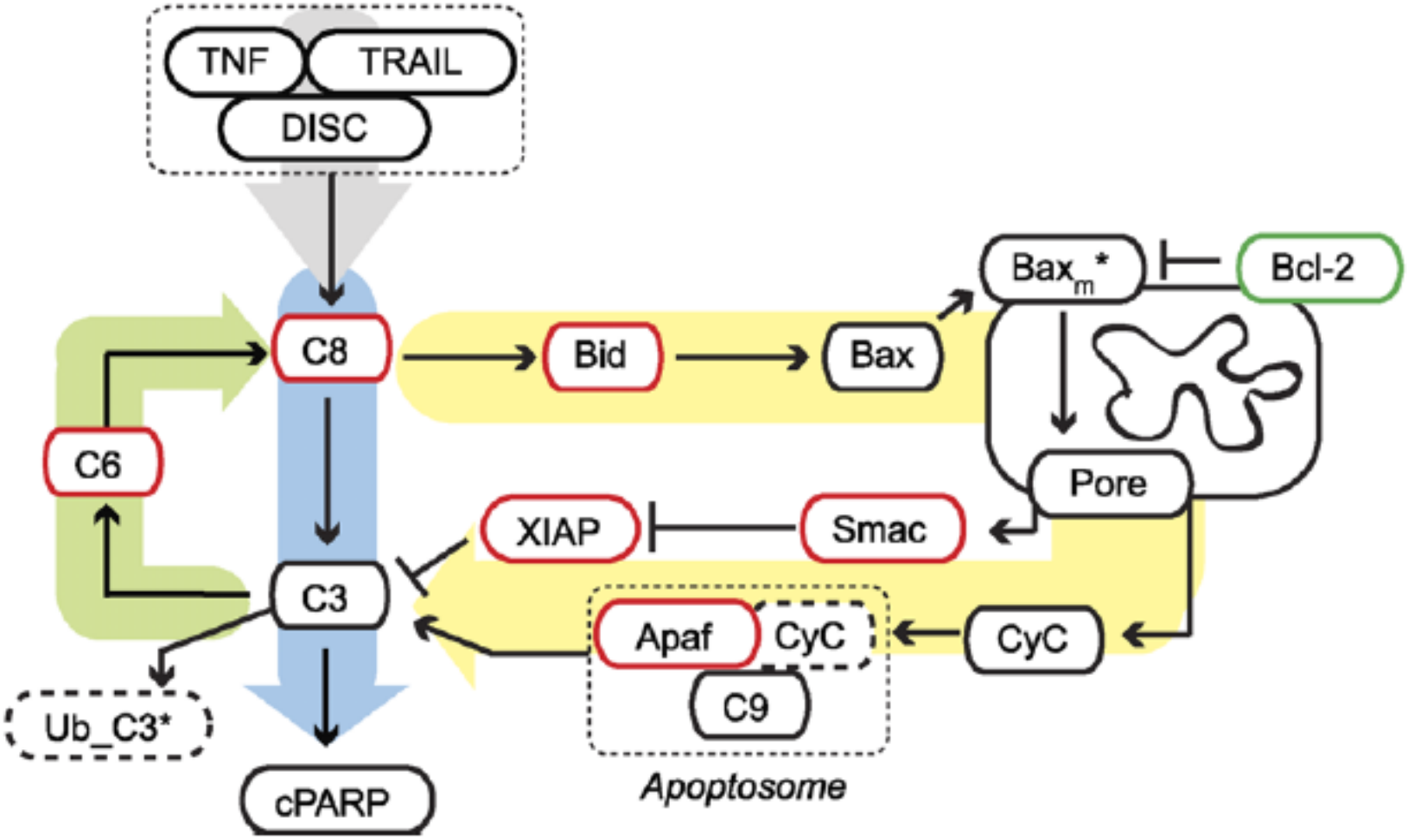

7. Prediction III: Snap-Action Switching Does Not Require Feedback

b. In simulation, inhibition of these feedback loops eliminates the second, rapid phase of IC-RP cleavage but has little effect on the dynamics of MOMP

c. Smac Knock-down experiments

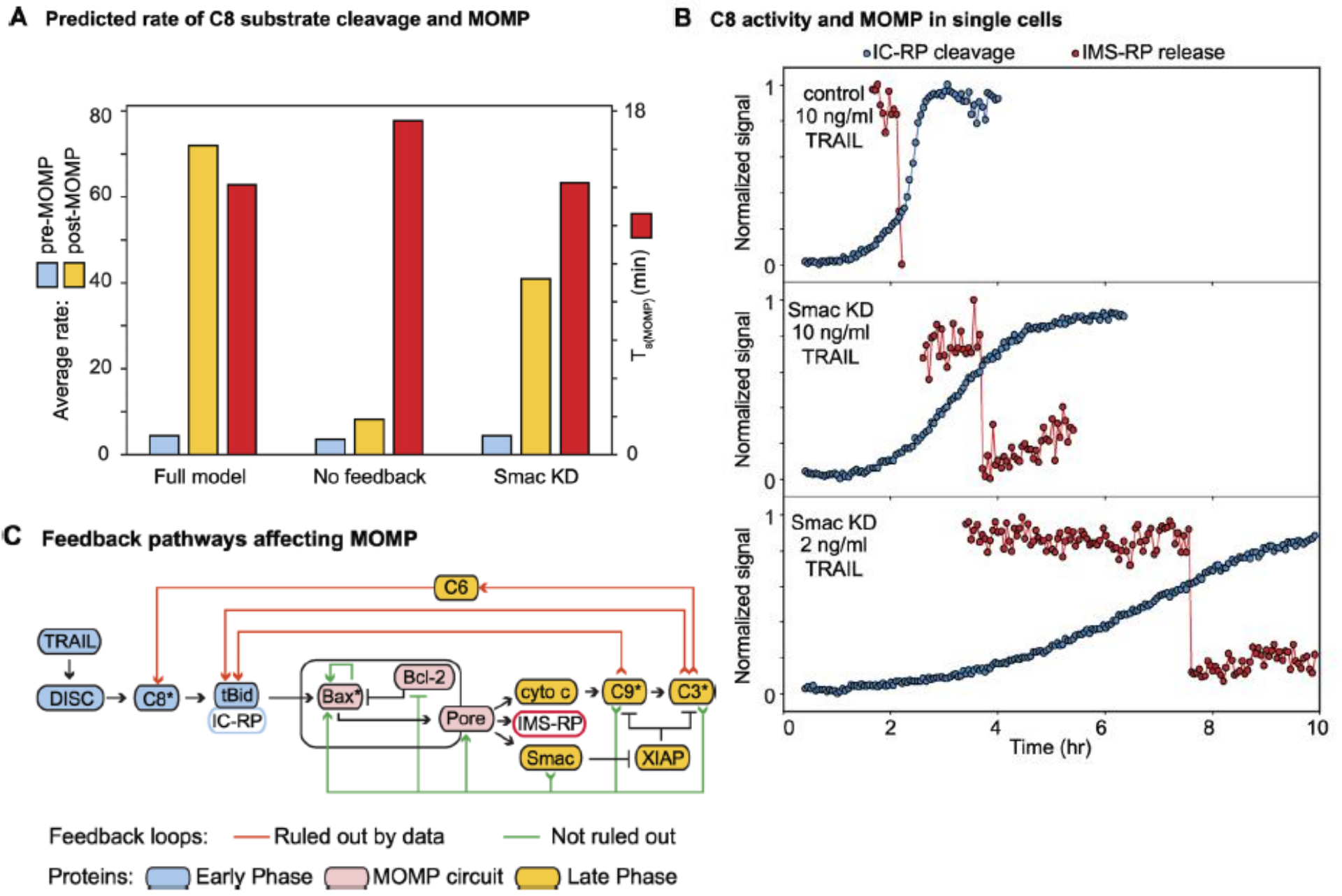

Figure 7. Rapid MOMP Independent of the Rapid Phase of Initiator Activity

8. Prediction IV: Dose-Dependent Activation of C8* Controls the Duration of Td

- Modeling suggests that the dose-dependence of Td is determined by the time required to saturate Bcl-2 with Bax* and thereby generate Bax* active in pore-formation.
- This depends on the rate at which tBid is generated by C8*
- They predict that Td is controlled by dose-dependent changes in C8* activity

Condensed representation

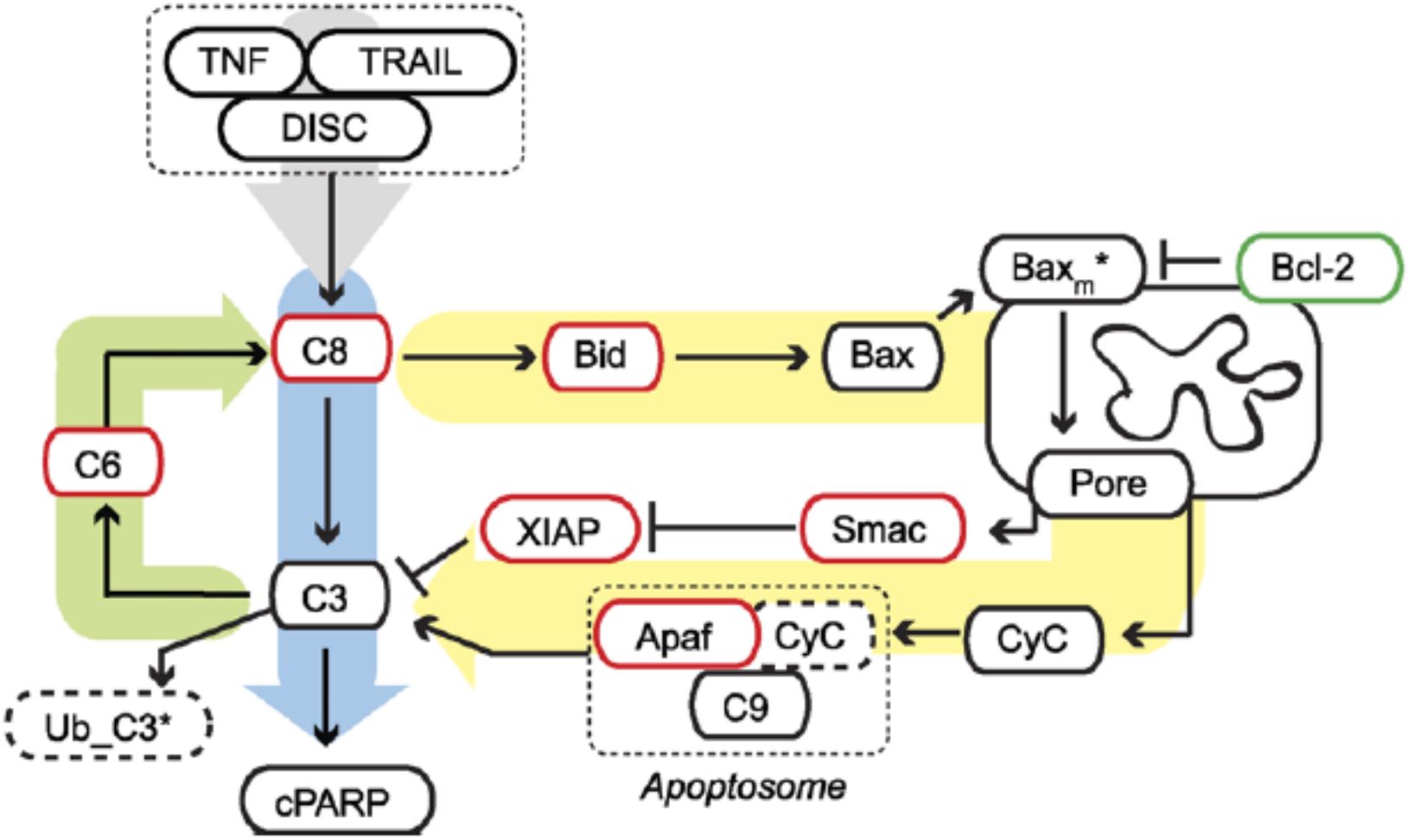

Figure 8. Control of Td by C8

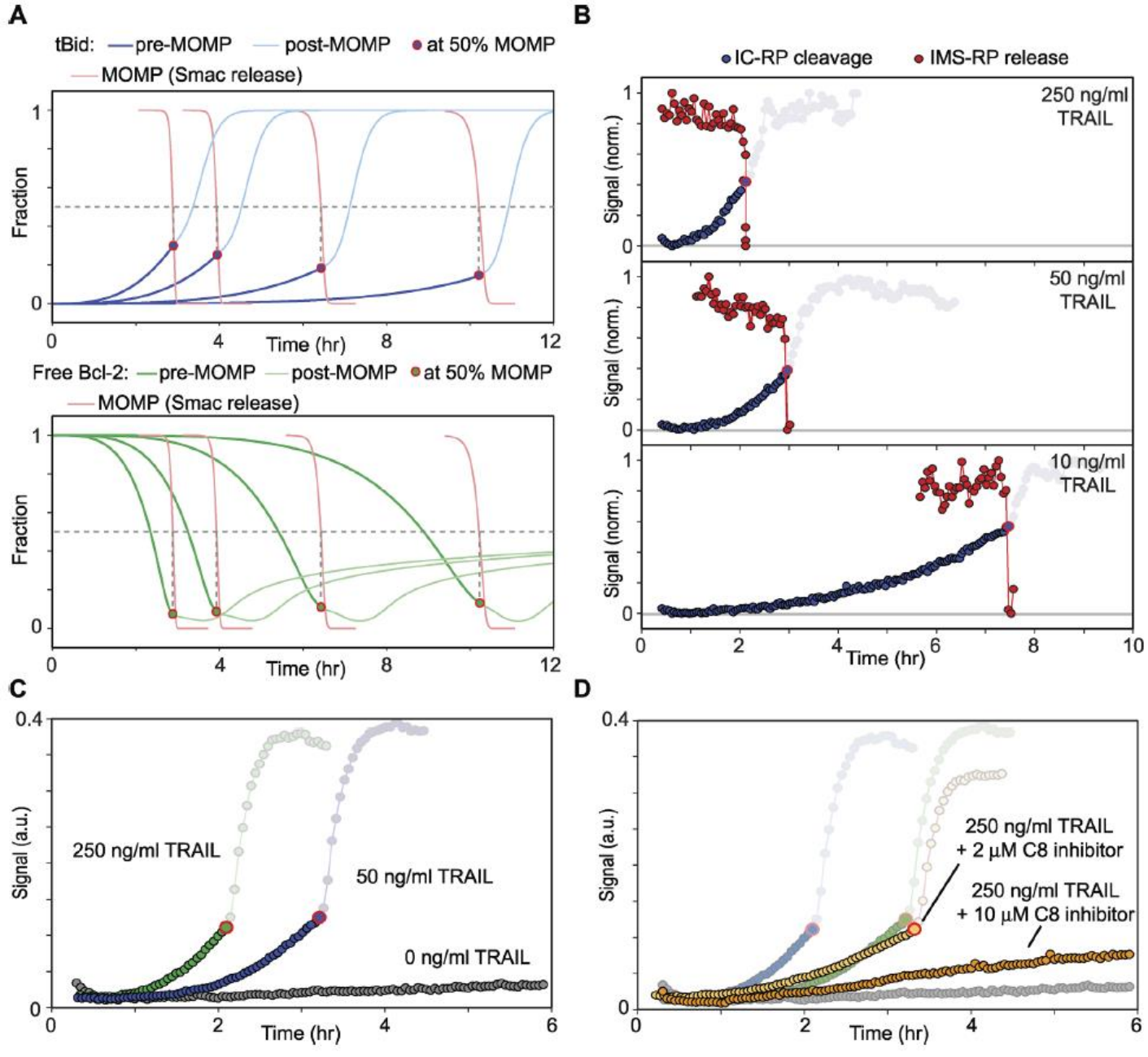

(A) Simulation of C8 substrate cleavage (tBid, top) and free mitochondrial Bcl-2 (bottom).
(B) Live-cell measurement of IC-RP cleavage and IMS-RP release in individual cells.
(C) Averaged IC-RP cleavage.
(D) Average IC-RP cleavage in Hela cell with 250 ng/ml TRAIL in the presence of C8 inhibitor.

9. Prediction V: Ratiometric Control of Snap-Action Transmission

- Two sets of reactions “transmit” the death signal generated by MOMP to C3*: (i) binding of cytosolic Smac to XIAP and (ii) assembly of the apoptosome
- hypothesize that the key quantity controlling signal transmission from MOMP to C3* is the ratio of XIAP to the sum of the Smac and apoptosome in the cytosol.
- Modeling prediction only. Not able to confirm this result with multiple Apaf-1 oligos

The network

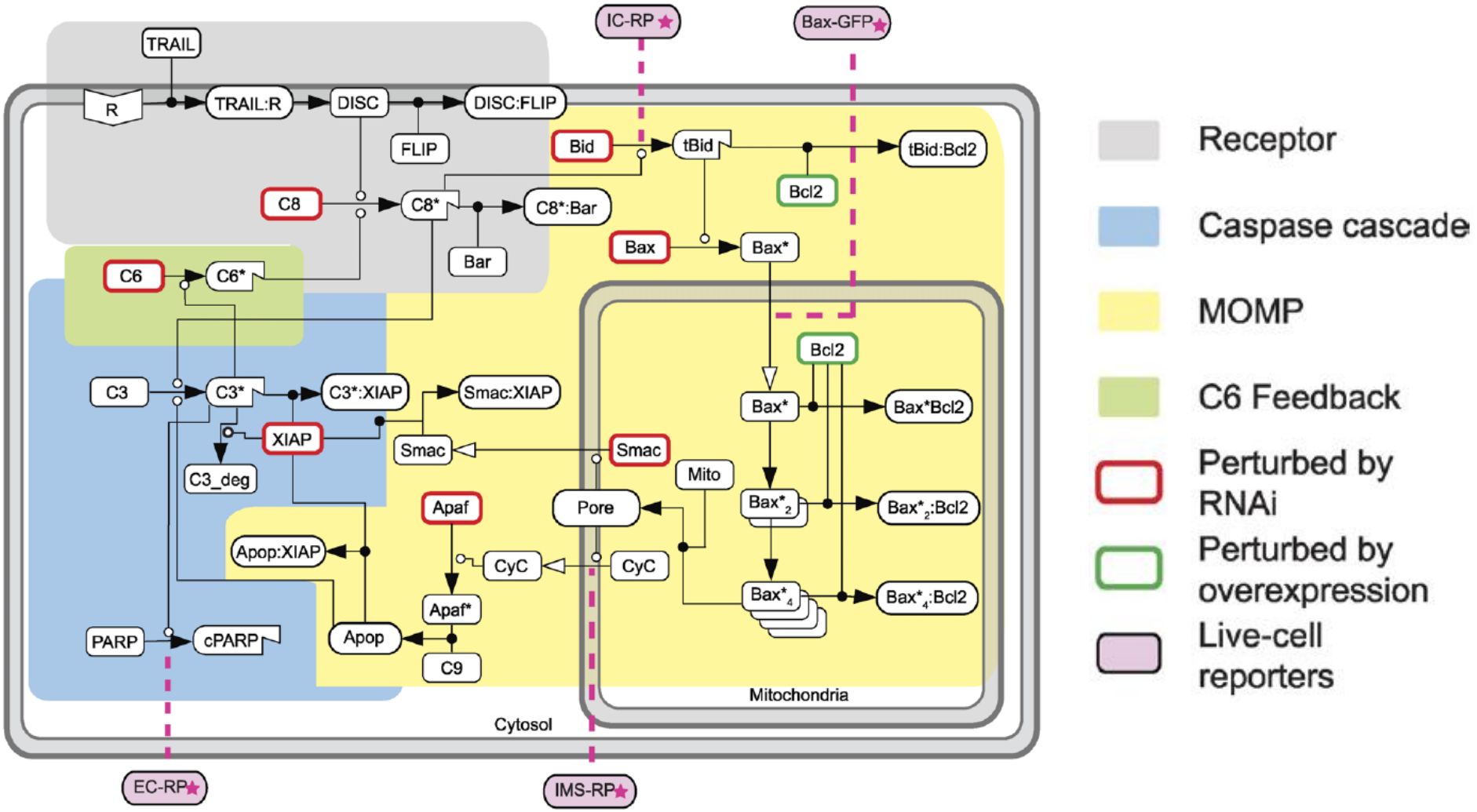

Simplifying: **C8**: C8 and C10; **C3**: C3 and C7;

Bcl-2 family: **Bid**: apoptotic ‘activator’; **Bcl-2**; apoptotic inhibitor

Bax: pore-forming protein

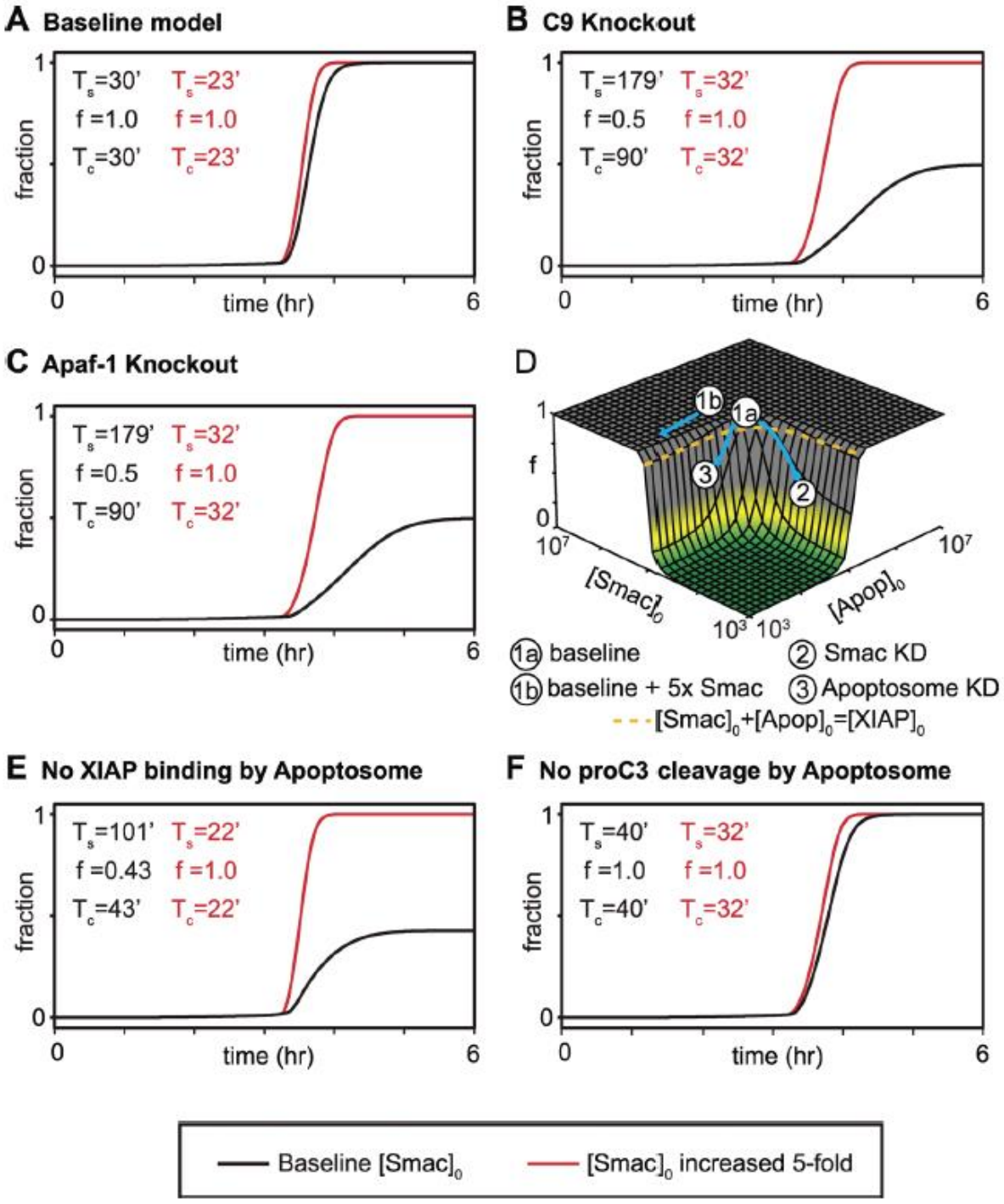

Figure 9. Role of the Apoptosome in Snap-Action C3 Activation.

(A–C) Simulation of the time course of C3 (EC) substrate cleavage in WT (A), or C9 deletion (B), or Apaf-1 deletion(C).

(D) Simulation of f as a function of initial concentrations of Smac and the apoptosome; for simplicity, the apoptosome components C9 and Apaf-1 were assumed to be present at equal concentrations.

(E, F) Simulation of the time course of PARP cleavage in cells in which apoptosome function has been altered so that it cannot process pro-C3 (E) or so that it cannot bind XIAP (F).

10. Prediction VI: C6*-Mediated Feedback Controls Td but Not Ts

- KD C6 has little effect on dynamics
- C8* have fast source (DISC) and slow source (C6*)
- At very low dose of TRAIL and minimum levels of DISC-generated C8*, C6* could generate enough C8* to control Td
- Experiments with Hela does not produce this scenario.

Condensed representation

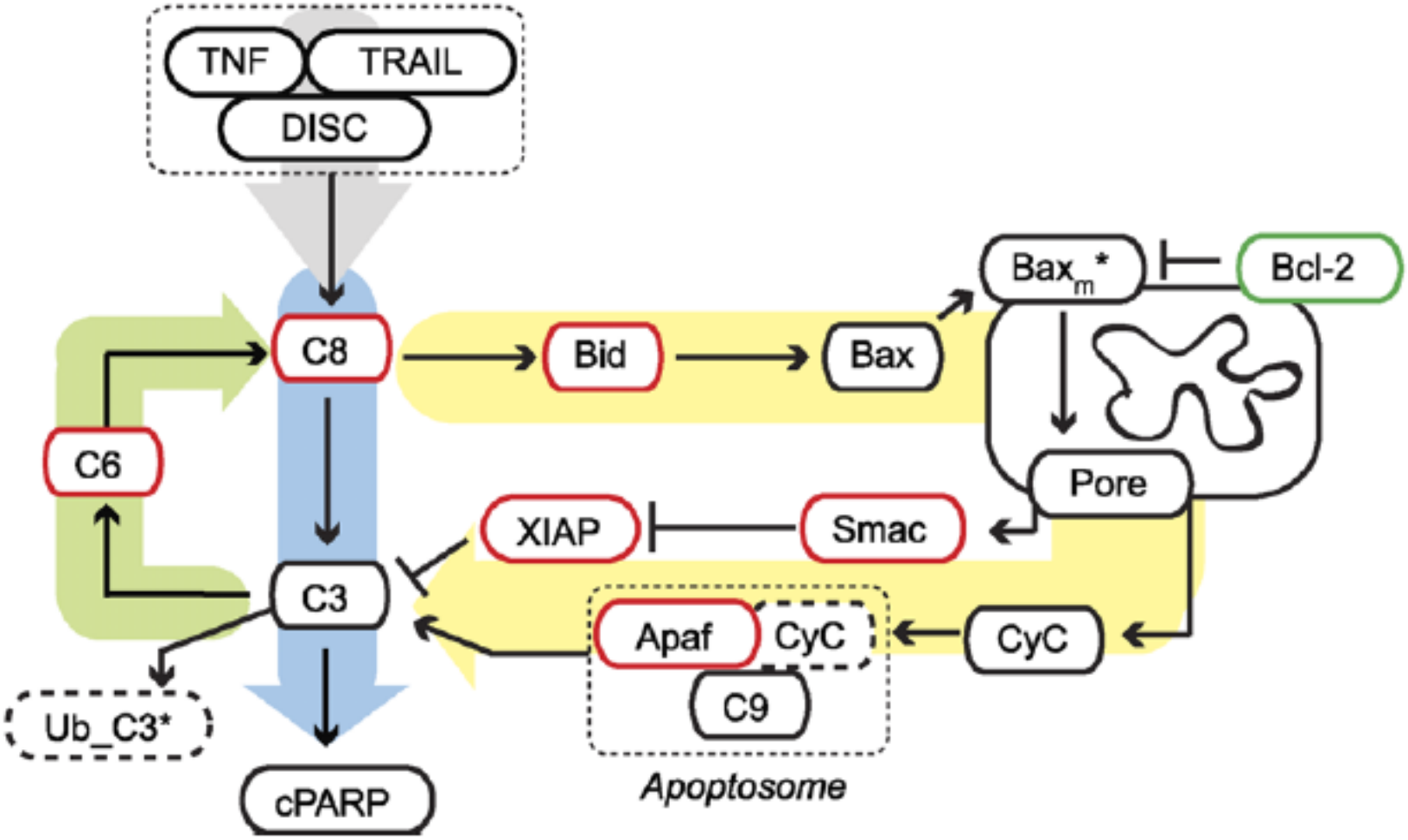

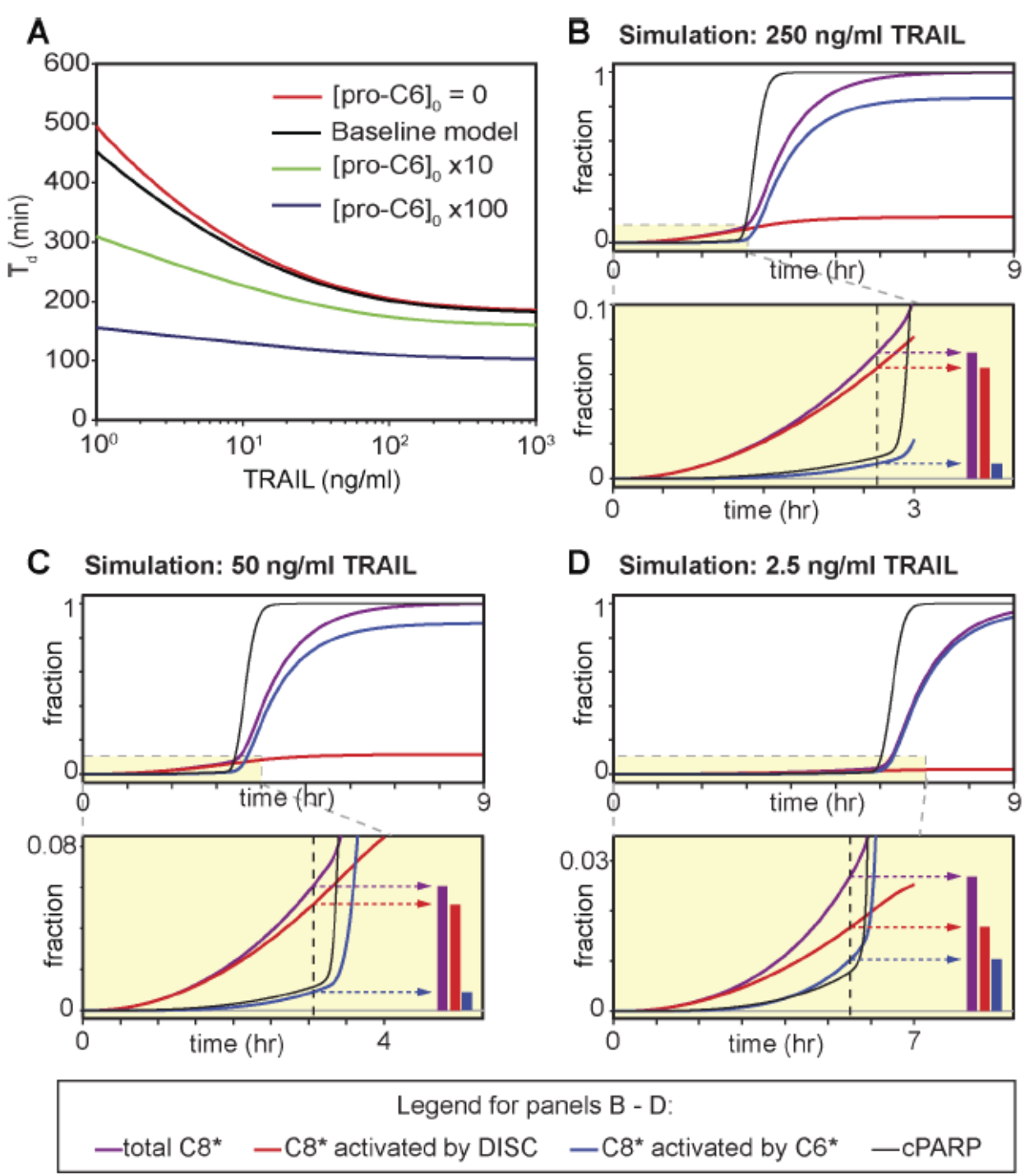

Figure 10. Role of C6 in Modulating the Duration of Pre-MOMP Delay (Td)

(A) Simulation showing the effect on Td of increasing the levels of $[C6]_0$.

(B–D) Simulations showing concentrations of total C8* and the subset of C8* generated by DISC or by C6* at three different doses of TRAIL.

The bottom panels magnify the period immediately before and after snap-action switching; bar plots to the right depict levels of DISC- or C6*-generated C8* (normalized to a total C8* value of 1.0) at the time of MOMP onset (dotted vertical lines).

11. Building a Threshold-Sensitive Snap-Action Switch

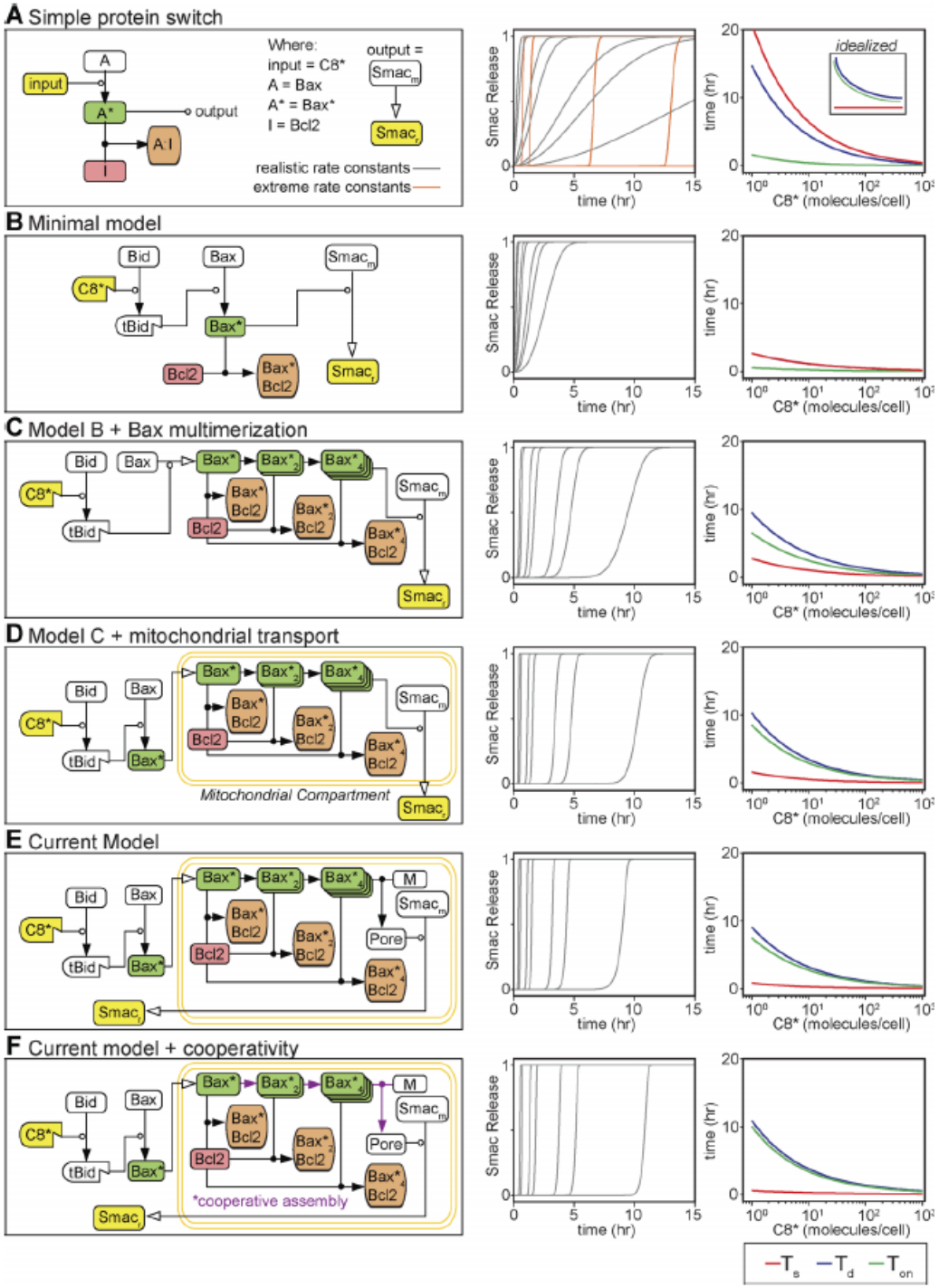

Figure 11. Role of Network Topology in Generating Snap-Action Behavior

Models representing varying topologies of the MOMP module were analyzed for snap-action behavior. (A) Basic motif model. The inset plot in the right column shows the expected behavior for an idealized variable-delay snap-action switch. (B) Model including Bid cleavage. (C) Model including Bax oligomerization. (D) Model including separate mitochondrial reaction compartment. (E) Model corresponding to the MOMP module in EARM v1.0.. (F) Model as in (F), but with rate constants for Bax oligomerization and insertion adjusted to represent positive cooperativity.

Conclusions: bite the bullet

- Modeling involves a tradeoff between tractability and detail or scope.
- Models spanning reactions upstream and downstream of MOMP yield insight that cannot be obtained from models having less scope.
- Significant mechanistic detail (e.g., multimerization, physical compartmentalization, etc.) was necessary to reproduce the features of TRAIL-induced MOMP identified experimentally.
- The importance of integrating modeling and experimentation is often emphasized, but is difficult to achieve in practice.
- The authors use data fusion and **simulation** to integrate measurements made by **live-cell imaging**, **flow cytometry**, and **immunoblotting**.

Conclusions:

- Determinants of Snap-Action Activation
  - MOMP
- Feedback and Network Bistability
  - Caspase-dependent feedback not important for Snap-action
- Determinants of Variable Delay
  - generate enough Bax* to exhaust the pool of mitochondrial Bcl-2
- Physiological Importance of Variable-Delay Snap-Action Switching
  - the rapidity of switching should prevent cells from initiating but failing to complete the cell death program
  - dose-dependent variation in Td should make it possible to regulate the strength of a death signal independent of an all-or-none response at the single-cell level
  - cell-to-cell variability in Td within a population, prevents cells from dying en masse following exposure to a death stimulus

The network

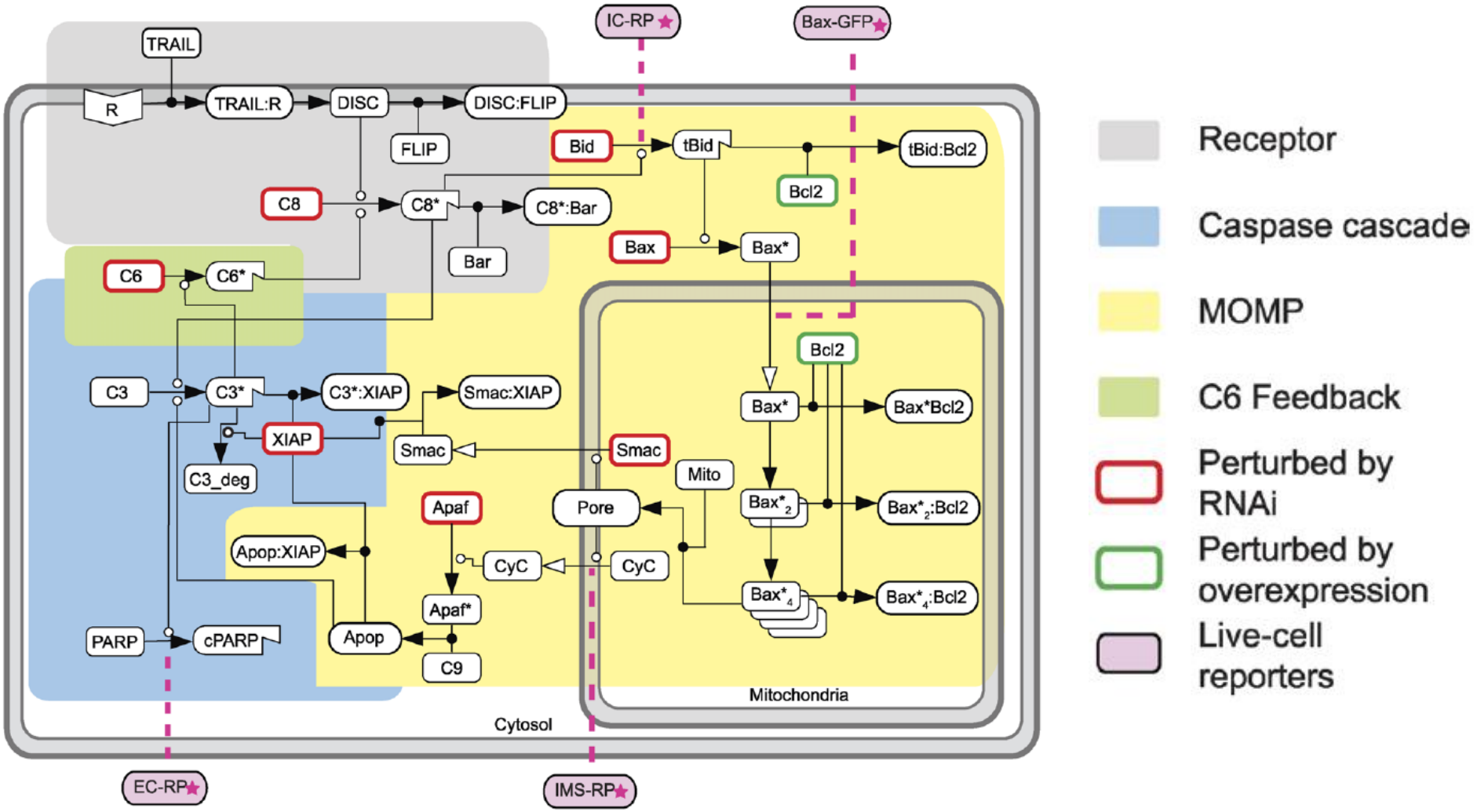

Simplifying: **C8**: C8 and C10; **C3**: C3 and C7;

Bcl-2 family: **Bid**: apoptotic ‘activator’; **Bcl-2**; apoptotic inhibitor

Bax: pore-forming protein